Analysis of charge transfer effects in molecular complexes based on absolutely localized molecular orbitals

Rustam Z. Khaliullin,[1,2,a)] Alexis T. Bell,[1,3] and Martin Head-Gordon[1,2]
[1]*Chemical Sciences Division, Lawrence Berkeley National Laboratory, Berkeley, California 94720, USA*
[2]*Department of Chemistry, University of California, Berkeley, California 94720, USA*
[3]*Department of Chemical Engineering, University of California, Berkeley, California 94720, USA*

(Received 10 December 2007; accepted 27 March 2008; published online 14 May 2008)

A new method based on absolutely localized molecular orbitals (ALMOs) is proposed to measure the degree of intermolecular electron density delocalization (charge transfer) in molecular complexes. ALMO charge transfer analysis (CTA) enables separation of the forward and backward charge transfer components for each pair of molecules in the system. The key feature of ALMO CTA is that all charge transfer terms have corresponding well defined energetic effects that measure the contribution of the given term to the overall energetic stabilization of the system. To simplify analysis of charge transfer effects, the concept of chemically significant complementary occupied-virtual orbital pairs (COVPs) is introduced. COVPs provide a simple description of intermolecular electron transfer effects in terms of just a few localized orbitals. ALMO CTA is applied to understand fundamental aspects of donor-acceptor interactions in borane adducts, synergic bonding in classical and nonclassical metal carbonyls, and multiple intermolecular hydrogen bonds in a complex of isocyanuric acid and melamine. These examples show that the ALMO CTA results are generally consistent with the existing conceptual description of intermolecular bonding. The results also show that charge transfer and the energy lowering due to charge transfer are not proportional to each other, and some interesting differences emerge which are discussed. Additionally, according to ALMO CTA, the amount of electron density transferred between molecules is significantly smaller than charge transfer estimated from various population analysis methods. © *2008 American Institute of Physics*. [DOI: 10.1063/1.2912041]

I. INTRODUCTION

Molecular complexes represent a broad class of systems with interesting chemical and physical properties controlled by the intermolecular interactions. Similarly, molecular interactions determine many important properties of liquids, solutions, and molecular solids. They govern physisorption in van der Waals systems and control self-assembly and self-organization processes in supramolecular systems.[1,2] Hydrogen bonding plays an important role in the chemistry of numerous systems, ranging from small water clusters to nanodroplets, bulk water, and solvated biomolecules.[3–7] Metal-ligand interactions give rise to a wide variety of metal complexes with different physical properties, chemical behavior, and numerous practical applications.[8,9] Many chemical reactions involve nondissociative molecular adsorption, formation of σ-complexes, and solvent-active site interactions.[10–12] These interactions directly affect reaction energetics and pathways.

The strength of intermolecular binding is inextricably connected to the fundamental nature of the interactions between molecules.[13] Intermolecular complexes can be stabilized through electrostatic effects (for example, charge-charge, charge-dipole, and charge-induced dipole interactions) and donor-acceptor type orbital interactions such as forward and backdonation of electron density between the molecules. Depending on the extent of these interactions, the intermolecular binding can vary in strength from just several kJ/mol (van der Waals complexes) to several hundred kJ/mol (metal-ligand bonds in metal complexes). Understanding the contributions of various interaction modes may enable one to tune the strength of the intermolecular binding to a target range by making appropriate chemical modifications.

The demand for a physically reasonable description of the intermolecular interaction components has resulted in numerous energy decomposition analysis (EDA) schemes over the years.[14–26] Most decomposition methods represent the total interaction energy as a sum of a frozen density interaction energy, a polarization energy, and charge transfer energy terms. The frozen density term is calculated as the interaction energy of the unrelaxed electron densities on the molecules allowing only for Pauli repulsion. The polarization term is due to the relaxation (or polarization) of the electron clouds of the molecules in the field of each other. Quantum mechanically, it can be described as the energy lowering due to the *intramolecular* relaxation of the molecular orbitals. Finally, the charge transfer can be pictured as the electron flow to and from each molecule in the system due to *intermolecular* relaxation (or mixing) of the molecular orbitals. Although quantitative values for charge transfer effects vary from one EDA scheme to another, all energy decomposition methods

[a)]Author to whom correspondence should be addressed: Electronic mail: rustam@khaliullin.com.

 © 2008 American Institute of Physics

Downloaded 26 Nov 2008 to 128.32.49.120. Redistribution subject to AIP license or copyright; see http://jcp.aip.org/jcp/copyright.jsp

give unequivocal evidence that they have significant weight in almost all types of intermolecular interactions. In this paper, we introduce a quantitative scale for measuring the degree of intermolecular electron density delocalization in molecular complexes and demonstrate a direct connection of such charge transfer effects to the energetic stabilization of the system.

To study electron density delocalization in molecular complexes, the system is usually partitioned into molecular subsystems in either three dimensional space or in Hilbert space. Methods such as the quantum theory of atoms in molecules,[27,28] the electron localization function,[29–31] and Hirshfeld analysis[32] are examples of topological methods that study the spatial distribution of scalar fields derived from reduced electron density matrices. In this work, we are concerned with methods based on partitioning Hilbert space. Existing examples include such popular methods as natural population analysis,[33] Mulliken population analysis (MPA),[34,35] Löwdin population analysis,[36] and many others.[37–40] In each method in this category, one-electron basis functions (orbitals) that span the supermolecular Hilbert space are assigned to individual molecules and the formal charge on a molecule is calculated as a sum of the *population* of all orbitals associated with the given molecule and its nuclear charges. To obtain the orbital population and thus the molecular formal charges, each method needs to specify a prescription for constructing basis functions and a procedure for treating the basis function overlap. In population analysis (PA) methods, the intermolecular charge transfer ΔQ can be inferred from the formal molecular charges (see Appendix).

In this paper, we present another way of measuring ΔQ in molecular complexes described by single-determinant wavefunctions [Hartree–Fock or density functional theory (DFT)]. We demonstrate that, unlike ΔQ inferred from PA methods, the intermolecular electron density transfer in our approach has a corresponding well defined energy of stabilization.

To isolate intermolecular charge transfer from electron density penetration effects (i.e., spatial overlap of the unrelaxed electron densities on the molecules) and from polarization effects (i.e., intramolecular charge reorganization in the field of the neighboring molecules), it is convenient to use an intermediate partially optimized wavefunction that (i) already includes frozen density interactions (spatial overlap), (ii) is variationally optimized to self-consistency to include polarization effects, and (iii) gives zero charge transfer between molecules according to some preselected population analysis method. Employing an intermediate state (wavefunction) to isolate intra- and intermolecular electron density reorganization effects makes such analysis closely related to EDA methods as the latter also require an intermediate state to separate the charge transfer energy from the rest of the energy terms. In this work, the reference intermediate state (wavefunction) is constructed from the variationally optimized absolutely localized molecular orbitals (ALMOs),[41–47] which have been recently used for energy decomposition methods by Mo *et al.*[25] (BLW EDA) and by Khaliullin *et al.* (ALMO EDA).[26] Unlike conventional MOs, which are generally delocalized over all molecules in the system, the ALMOs are expanded in terms of the atomic orbitals (AOs) of only a given molecule.[25,26,41,42,44,45] It can be shown that the MPA gives zero charge transfer between molecules for any one-electron density matrix constructed from ALMOs. Therefore, the state constructed from variationally optimized ALMOs (i.e., polarized ALMOs)[25,26] satisfies conditions (i)–(iii). Its main advantage over other ALMO states is a fully self-consistent treatment of polarization effects. Thus, the polarized ALMO state is particularly useful to study charge transfer effects in molecular complexes. The self-consistent field procedure for the variational optimization of the ALMOs (i.e., for finding the polarized ALMO state) is called SCF for molecular interactions, or SCF MI, and its mathematical and algorithmic details has been described by many authors.[41,42,44,45]

It has been recently shown[26] that the charge transfer energy term in the ALMO EDA can be separated into forward and backdonation components using a perturbative Roothaan step (RS) approximation starting from the optimized ALMO reference. In this paper, we show that a similar formulation can also be used to separate ΔQ into bonding and backbonding components for each pair of molecules in the complex. The charge decomposition analysis (CDA) method of Dapprich and Frenking[48] also defined forward donation and backbonding components of intermolecular charge transfer. The simplicity and the ease of implementation of CDA have made this method popular for estimating the amount of the electron delocalization in donor-acceptor complexes. However, as mentioned in the original CDA paper,[48] this definition of charge transfer should not be confused with "physical interpretation of chemical bonding." As shown in the Appendix, some terms in CDA do not have a clear physical meaning. We examine the results obtained with the CDA method and compare them to the results of our ALMO-based charge transfer analysis (ALMO CTA).

In addition to quantifying the amount and energetics of intermolecular charge transfer, it is often useful to have a simple description of *orbital* interactions in intermolecular complexes. The natural bond orbital (NBO) analysis of donor-acceptor complexes has gained wide popularity because of its ability to provide such an orbital interaction picture.[49] In this paper, we demonstrate how the ALMO approach can be used to construct a conceptually simple orbital interaction model. The polarized ALMOs obtained from the SCF MI procedure and used as a reference basis set in the decomposition analysis do not directly show which occupied-virtual orbital pairs are of most importance in forming intermolecular bonds. We demonstrate that, by performing rotations of the polarized ALMOs within a molecule, it is possible to find a "chemist's basis set" that represents bonding between molecules in terms of just a few localized orbitals. This orbital interaction model validates existing conceptual descriptions of intermolecular bonding. For example, in the modified ALMO basis, donor-acceptor bonding in ammonia borane ($H_3N–BH_3$) is represented as the lone orbital pair on the nitrogen atom donating electrons to the empty orbital on the boron atom, and the description of synergic bonding in metal complexes agrees well with simple Dewar–Chatt–Duncanson model.[50,51]

Downloaded 26 Nov 2008 to 128.32.49.120. Redistribution subject to AIP license or copyright; see http://jcp.aip.org/jcp/copyright.jsp

Summarizing, in this paper, we propose a new scale to measure intermolecular charge transfer effects in molecular complexes. We also show how to separate the total charge transfer term into forward and backdonation components for each pair of molecules in the system. Finally, we propose a method to construct chemically significant orbitals localized on molecules that provide a simple chemical description of intermolecular interactions. In addition, we demonstrate that each charge transfer term defined in this work has a corresponding energy lowering that measures the contribution of the given term to the overall energetic stabilization of the system. Thus, the ALMO-based method proposed here unifies energy decomposition analysis, charge transfer decomposition analysis, and orbital-orbital interaction analysis for molecular systems.

To demonstrate the validity and usefulness of the new ALMO-based charge transfer analysis based on the absolutely localized molecular orbitals (ALMO CTA), we applied it to a series of problems of chemical interest:

- donor-acceptor interactions in borane adducts;
- synergic bonding in classical and nonclassical metal carbonyls; and
- multiple intermolecular hydrogen bonds in a complex of isocyanuric acid and melamine.

We show that the ALMO CTA results are generally consistent with the existing conceptual pictures of intermolecular bonding and agree with the ALMO energy decomposition analysis. We hope that the ALMO approach reported in this paper will become a useful theoretical tool for studying and analyzing binding mechanisms in molecular complexes.

II. THEORY

A. Summary of the ALMO energy decomposition analysis

Energy decomposition methods based on ALMOs have been proposed by Mo *et al.*[25] (BLW EDA) and by Khaliullin *et al.* (ALMO EDA).[26] In these methods, the overall binding energy is decomposed into frozen density component (FRZ), polarization (POL), and charge transfer (CT) terms

$$\Delta E_{\mathrm{TOTAL}} = \Delta E_{\mathrm{FRZ}} + \Delta E_{\mathrm{POL}} + \Delta E_{\mathrm{CT}}. \tag{1}$$

The frozen density term (FRZ) is defined as the SCF energy change that corresponds to bringing infinitely separated molecules into the complex geometry without any relaxation of the MOs on the monomers (apart from changes associated with satisfying the Pauli principle).

$$\Delta E_{\mathrm{FRZ}} \equiv E_{\mathrm{SCF}}(\hat{R}_{\mathrm{FRZ}}) - \sum_{x} E_{\mathrm{SCF}}(\hat{R}_{x}), \tag{2}$$

where $E_{\mathrm{SCF}}(\hat{R}_x)$ is the SCF energy of the variationally optimized one-electron density matrix of the isolated molecule x with its nuclei fixed at the complex geometry and $\hat{R}_{\mathrm{FRZ}}$ is the density matrix of the complex constructed from the unrelaxed nonorthogonal occupied MOs of the molecules [see Eq. (8) below].

The polarization energy is defined as the energy lowering due to intramolecular relaxation of each molecule's absolutely localized MOs in the field of all other molecules in the system. The intramolecular relaxation is constrained to include only variations that keep MOs localized on their molecule:

$$\Delta E_{\mathrm{POL}} \equiv E_{\mathrm{SCF}}(\hat{R}_{\mathrm{POL}}) - E_{\mathrm{SCF}}(\hat{R}_{\mathrm{FRZ}}), \tag{3}$$

where $\hat{R}_{\mathrm{POL}}$ is the density matrix constructed from the fully optimized (polarized) ALMOs according to Eq. (8). According to the Mulliken PA, the ALMO expansion explicitly excludes charge transfer from one molecule to another. Mathematical details of the SCF procedure for finding the polarized state $\hat{R}_{\mathrm{POL}}$ are given elsewhere.[41]

The remaining portion of the total interaction energy, the CT energy term, is calculated as the energy difference between the state formed from the fully relaxed ALMOs, $\hat{R}_{\mathrm{pol}}$, and the state constructed from the fully optimized delocalized MOs, $\hat{R}_{\mathrm{SCF}}$.

$$\Delta E_{\mathrm{CT}} \equiv E_{\mathrm{SCF}}(\hat{R}_{\mathrm{SCF}}) - E_{\mathrm{SCF}}(\hat{R}_{\mathrm{POL}}), \tag{4}$$

where ΔE_{CT} includes the energy lowering due to electron transfer from occupied orbitals on one molecule to virtual orbitals of another molecule as well as the further energy change caused by induction (or repolarization) that accompanies such an occupied-virtual mixing. In the ALMO EDA of Khaliullin *et al.*, the energy lowering of the occupied-virtual excitations (mixing) is described with a single noniterative RS correction starting from the converged ALMO solution.[26,41] The remaining higher order (HO) relaxation term includes all induction effects that accompany occupied-virtual charge transfer and is generally small,

$$\Delta E_{\mathrm{CT}} = \Delta E_{\mathrm{CT}}^{\mathrm{RS}} + \Delta E_{\mathrm{CT}}^{\mathrm{HO}}. \tag{5}$$

Most importantly, for the purpose of the energy decomposition analysis, the mathematical form of the RS energy expression allows one to decompose the occupied-virtual mixing term into forward and backdonation components for each pair of molecules in the complex,

$$\Delta E_{\mathrm{CT}}^{\mathrm{RS}} = \sum_{x,y<x} \{\Delta E_{x\to y}^{\mathrm{RS}} + \Delta E_{y\to x}^{\mathrm{RS}}\}. \tag{6}$$

The HO energy contribution cannot be naturally divided into forward and backdonation terms.[26]

Thus, the four states—$\hat{R}_{\mathrm{FRZ}}$, $\hat{R}_{\mathrm{POL}}$, $\hat{R}_{\mathrm{RS}}$, and $\hat{R}_{\mathrm{SCF}}$—define energy terms in the ALMO EDA. The $\hat{R}_{\mathrm{pol}}$ state is the lowest energy state that can be constructed from completely localized molecular orbitals. Naturally, the electron density relaxation from $\hat{R}_{\mathrm{POL}}$ to $\hat{R}_{\mathrm{SCF}}$ provides a measure for intermolecular charge transfer effects ΔQ in the system.

B. Notation

We denote polarized ALMOs as $|\psi_{xp}\rangle$. The first index indicates that this orbital is localized on (or assigned to) molecule x, and the second index refers to the number of the orbital within the molecular subset. Latin letters $x-z$ are for the molecular indices, letters $i-k$ are used to label occupied

Downloaded 26 Nov 2008 to 128.32.49.120. Redistribution subject to AIP license or copyright; see http://jcp.aip.org/jcp/copyright.jsp

orbitals, $a-c$ denote virtual orbitals, and $p-t$ correspond to generic (occupied and virtual) orbitals. O and V refer to the number of occupied and virtual basis functions in the system, respectively, N is the total number of MOs in the system. o_x, v_x, and n_x correspond to the number of occupied, virtual, and total MOs on molecule x, respectively.

ALMOs are not orthogonal from one molecule to the next and their overlap is denoted as $\sigma_{xp,yq}=\langle\psi_{xp}|\psi_{yq}\rangle$. The biorthogonal basis function are denoted with superscripts,

$$|\psi^{xp}\rangle=\sum_{yq}^{N}|\psi_{yq}\rangle(\sigma^{-1})_{yq,xp}. \tag{7}$$

The one-electron density operator constructed from the polarized ALMOs represents the projector onto the occupied subspace and is given by

$$\hat{R}\equiv\hat{R}_{\mathrm{POL}}=\sum_{xi,yj}^{O}|\psi_{xi}\rangle(\sigma_o^{-1})_{xi,yj}\langle\psi_{yj}|=\sum_{xi}^{O}|\psi_{xi}\rangle\langle\psi^{\bar{x}i}|, \tag{8}$$

where (σ_o^{-1}) is the inverse of the $O\times O$ overlap matrix of occupied basis functions and should not be confused with (σ^{-1}). Biorthogonal functions in the occupied subspace are constructed as follows:

$$|\psi^{\bar{x}i}\rangle=\sum_{yj}^{O}|\psi_{yj}\rangle(\sigma_o^{-1})_{yj,xi}. \tag{9}$$

To simplify our notation, we denote $\hat{R}_{\mathrm{POL}}$ with $\hat{R}$ throughout the paper. It is also convenient to define projector onto the virtual subspace $\hat{Q}$, the orthogonal complement of $\hat{R}$,

$$\hat{Q}=\hat{1}-\hat{R}=\sum_{xa,yb}^{V}|\tilde{\psi}_{xa}\rangle(\tilde{\sigma}_v^{-1})_{xa,yb}\langle\tilde{\psi}_{yb}|=\sum_{xa}^{V}|\tilde{\psi}_{xa}\rangle\langle\tilde{\psi}^{\bar{x}a}|, \tag{10}$$

where projected virtual orbitals $|\tilde{\psi}_{ya}\rangle$ span the virtual subspace and are orthogonal to the occupied orbitals,

$$|\tilde{\psi}_{ya}\rangle=(\hat{1}-\hat{R})|\psi_{ya}\rangle=|\psi_{ya}\rangle-\sum_{xi}^{O}|\psi^{\bar{x}i}\rangle\sigma_{xi,ya}. \tag{11}$$

These definitions use the $V\times V$ overlap matrix of projected virtual orbitals,

$$(\tilde{\sigma}_v)_{xa,yb}=\langle\tilde{\psi}_{xa}|\tilde{\psi}_{yb}\rangle. \tag{12}$$

The biorthogonal basis in the virtual subspace is defined according to the following equation:

$$|\tilde{\psi}^{\bar{x}a}\rangle=\sum_{yb}^{V}|\tilde{\psi}_{yb}\rangle(\tilde{\sigma}_v^{-1})_{yb,xa}. \tag{13}$$

C. ALMO charge transfer analysis

The electron density reorganization from an initial state $\hat{R}_s$ to a final state $\hat{R}_f$ is defined as the amount of the electron density that, in the final state, occupies the initially unoccupied subspace. Such a reorganization term is given by the following equation:

$$\Delta Q_{(s\to f)}=\mathrm{Tr}[\hat{Q}_s\hat{R}_f\hat{Q}_s]=-\mathrm{Tr}[\hat{R}_s\hat{R}_f\hat{R}_s-\hat{R}_s], \tag{14}$$

where $\hat{Q}_s=\hat{1}-\hat{R}_s$ is the projector onto the initially unoccupied (virtual) subspace. Note that positive values of ΔQ correspond to the negative charge being transferred.

As mentioned in the ALMO EDA section, intermolecular charge transfer effects are measured as the change from the polarized ALMO state to the fully converged SCF state,

$$\Delta Q_{\mathrm{CT}}\equiv\Delta Q_{(\mathrm{POL}\to\mathrm{SCF})}. \tag{15}$$

In agreement with ALMO EDA, the charge transfer due to occupied-virtual mixing ($\Delta Q_{\mathrm{CT}}^{\mathrm{RS}}$) and the accompanying higher order relaxation terms ($\Delta Q_{\mathrm{CT}}^{\mathrm{HO}}$) are defined as follows:

$$\Delta Q_{\mathrm{CT}}^{\mathrm{RS}}\equiv\Delta Q_{(\mathrm{POL}\to\mathrm{RS})}, \tag{16}$$

$$\Delta Q_{\mathrm{CT}}^{\mathrm{HO}}\equiv\Delta Q_{\mathrm{CT}}-\Delta Q_{\mathrm{CT}}^{\mathrm{RS}}. \tag{17}$$

These definitions of $\Delta Q_{\mathrm{CT}}^{\mathrm{RS}}$ and $\Delta Q_{\mathrm{CT}}^{\mathrm{HO}}$ enable one to assign an energy lowering to each intermolecular electron transfer term. Since the Mulliken PA gives zero charge transfer between molecules, ΔQ_{FRZ} and ΔQ_{POL} terms do not contribute to intermolecular electron density transfer.

In the ALMO EDA, the single RS perturbation theory is used to account for the energy lowering due to the occupied-virtual mixing $\Delta E_{\mathrm{CT}}^{\mathrm{RS}}$. We will show now how the corresponding charge transfer term $\Delta Q_{\mathrm{CT}}^{\mathrm{RS}}$ is calculated.

The RS is the search for the unitary operator $\hat{U}$ that minimizes the energy functional

$$E[\hat{U}]=\mathrm{Tr}[\hat{F}\hat{U}\hat{R}\hat{U}^{\dagger}], \tag{18}$$

where $\hat{R}=\hat{R}_{\mathrm{POL}}$ and $\hat{F}$ is the Fock operator constructed from the polarized ALMOs. The post RS (transformed) operators are given by

$$\hat{R}'\equiv\hat{R}_{\mathrm{RS}}=\hat{U}\hat{R}\hat{U}^{\dagger} \tag{19}$$

and

$$\hat{F}'=\hat{U}^{\dagger}\hat{F}\hat{U}. \tag{20}$$

Then, the RS energy lowering can be written as follows:

$$\Delta E_{\mathrm{CT}}^{\mathrm{RS}}=\mathrm{Tr}[\hat{R}\hat{F}'\hat{R}-\hat{R}\hat{F}\hat{R}]. \tag{21}$$

By using definition of $\Delta Q_{\mathrm{CT}}^{\mathrm{RS}}$ [Eq. (16)] and the general expression for charge reorganization [Eq. (14)], we have

$$\Delta Q_{\mathrm{CT}}^{\mathrm{RS}}=-\mathrm{Tr}[\hat{R}\hat{R}'\hat{R}-\hat{R}]. \tag{22}$$

There is a direct similarity between the RS energy [Eq. (21)] and charge [Eq. (22)] expressions. In the ALMO EDA, the energy term can be readily decomposed into bonding and backbonding components for each pair of molecules in the complex [Eq. (6)]. Here, we show how a similar approach can be used to isolate bonding and backbonding components of the charge transfer term. To do that, it is convenient to rewrite Eqs. (21) and (22) in terms of the excitation operator $\hat{X}$. First, we demonstrate how the energy equation can be rewritten (original derivation is given by Liang and Head-Gordon[52]) and then show how similar results can be obtained for the charge expression.

Downloaded 26 Nov 2008 to 128.32.49.120. Redistribution subject to AIP license or copyright; see http://jcp.aip.org/jcp/copyright.jsp

Equation (20) can be written as $\hat{F}\hat{U}=\hat{U}\hat{F}'$ and then pre- and postmultiplied by $\hat{R}$ to obtain

$$(\hat{R}\hat{F}\hat{R})(\hat{R}\hat{U}\hat{R})+(\hat{R}\hat{F}\hat{Q})(\hat{Q}\hat{U}\hat{R}) = (\hat{R}\hat{U}\hat{R})(\hat{R}\hat{F}'\hat{R})+(\hat{R}\hat{U}\hat{Q})(\hat{Q}\hat{F}'\hat{R}). \quad (23)$$

The last term in the right-hand side of Eq. (23) is zero since the minimization of the energy functional [Eq. (18)] is equivalent to finding $\hat{U}$ that nullifies the virtual-occupied block of the transformed Fock operator: $\hat{Q}\hat{F}'\hat{R}=0$. Equation (23) is then premultiplied by $(\hat{R}\hat{U}\hat{R})^{-1}$

$$(\hat{R}\hat{U}\hat{R})^{-1}(\hat{R}\hat{F}\hat{R})(\hat{R}\hat{U}\hat{R})+(\hat{R}\hat{U}\hat{R})^{-1}(\hat{R}\hat{F}\hat{Q})(\hat{Q}\hat{U}\hat{R})=\hat{R}\hat{F}'\hat{R}. \quad (24)$$

The obtained expression for $\hat{R}\hat{F}'\hat{R}$ is plugged into Eq. (21), and the terms inside the trace are rearranged as follows:

$$\Delta E_{\mathrm{CT}}^{\mathrm{RS}}=\mathrm{Tr}[(\hat{R}\hat{F}\hat{Q})(\hat{Q}\hat{U}\hat{R})(\hat{R}\hat{U}\hat{R})^{-1}]. \quad (25)$$

Defining a new operator as

$$\hat{X}\equiv\hat{Q}\hat{U}\hat{R}(\hat{R}\hat{U}\hat{R})^{-1}, \quad (26)$$

we have the following equation for the Roothaan step energy lowering:

$$\Delta E_{\mathrm{CT}}^{\mathrm{RS}}=\mathrm{Tr}[\hat{R}\hat{F}\hat{Q}\hat{X}]. \quad (27)$$

It can be shown that the newly defined operator $\hat{X}$ represents a Cayley generator of unitary transformation $\hat{U}$,[53]

$$\hat{U}=(\hat{1}+\hat{X}-\hat{X}^{\dagger})(\hat{1}+\hat{X}^{\dagger}\hat{X}+\hat{X}\hat{X}^{\dagger})^{-1/2}, \quad (28)$$

and is directly related to the first-order transformation of the zero-order orbitals

$$\hat{U}=\hat{1}+\hat{X}-\hat{X}^{\dagger}+O(\hat{X}^2). \quad (29)$$

Operator $\hat{X}$ satisfies the projection relation $\hat{X}=\hat{Q}\hat{X}\hat{R}$ by definition. Therefore, the ALMO occupied orbitals are mixed only with the zero-order virtual orbitals upon first-order transformation [Eq. (29)]. Thus, operator $\hat{X}$ is referred to as excitation operator and its matrix elements represent excitation amplitudes from the occupied to the virtual orbitals.

The excitation amplitudes can be found by solving the following single RS quadratic equation:[53]

$$\hat{Q}\hat{F}\hat{R}+\hat{Q}\hat{F}\hat{Q}\hat{X}\hat{R}-\hat{Q}\hat{X}\hat{R}\hat{F}\hat{R}-\hat{Q}\hat{X}\hat{R}\hat{F}\hat{Q}\hat{X}\hat{R}=0. \quad (30)$$

The operator $\hat{X}$ obtained from this equation gives the RS energy lowering that is equvalent to the result of single Fock matrix diagonalization or to the infinite-order single excitation perturbation theory result.[41,52,53]

We can express $\Delta Q_{\mathrm{CT}}^{\mathrm{RS}}$ in terms of the excitation operator $\hat{X}$. First, equation $\hat{R}'\hat{U}=\hat{U}\hat{R}$ is pre- and postmultiplied by $\hat{R}$:

$$(\hat{R}\hat{R}'\hat{R})(\hat{R}\hat{U}\hat{R})+(\hat{R}\hat{R}'\hat{Q})(\hat{Q}\hat{U}\hat{R})=\hat{R}\hat{U}\hat{R}, \quad (31)$$

and then the resulting Eq. (31) is postmultiplied by $(\hat{R}\hat{U}\hat{R})^{-1}$:

$$\hat{R}\hat{R}'\hat{R}=\hat{R}-(\hat{R}\hat{R}'\hat{Q})(\hat{Q}\hat{U}\hat{R})(\hat{R}\hat{U}\hat{R})^{-1}. \quad (32)$$

Next, the obtained expression for $\hat{R}\hat{R}'\hat{R}$ is substituted into Eq. (22) and is simplified by using the definition of the excitation operator [Eq. (26)]:

$$\Delta Q_{\mathrm{CT}}^{\mathrm{RS}}=\mathrm{Tr}[\hat{R}\hat{R}'\hat{Q}\hat{X}]. \quad (33)$$

Equation (33) gives the total amount of charge transfer from the occupied subspace to the virtual subspace of $\hat{R}\equiv\hat{R}_{\mathrm{pol}}$ when this state is relaxed to $\hat{R}'\equiv\hat{R}_{\mathrm{RS}}$. Equation (27) gives the energy lowering associated with this charge transfer.

In the next step, we partition the total charge transfer into the pairwise contributions assigned to electron flow from an individual occupied orbital to an individual virtual orbital. To do this, we introduce a set of partition operators, each corresponding to an occupied ($\hat{P}_{xi}$) or to a virtual ($\hat{P}_{xa}$) orbital. These operators must satisfy the resolution of identity property

$$\sum_{xi}^{O}\hat{P}_{xi}=\hat{R}, \quad (34)$$

$$\sum_{xa}^{V}\hat{P}_{xa}=\hat{Q}, \quad (35)$$

and the idempotency property

$$\hat{P}_{xi}^2=\hat{P}_{xi}, \quad (36)$$

$$\hat{P}_{xa}^2=\hat{P}_{xa}. \quad (37)$$

Using these partition operators, we define charge transfer from orbital xi to orbital ya and its corresponding energy as follows:

$$\Delta Q_{xi\rightarrow ya}^{\mathrm{RS}}=\mathrm{Tr}[\hat{P}_{xi}\hat{R}'\hat{P}_{ya}\hat{X}], \quad (38)$$

$$\Delta E_{xi\rightarrow ya}^{\mathrm{RS}}=\mathrm{Tr}[\hat{P}_{xi}\hat{F}\hat{P}_{ya}\hat{X}]. \quad (39)$$

Charge transfer from molecule x to molecule y and its energy are then expressed as

$$\Delta Q_{x\rightarrow y}^{\mathrm{RS}}=\sum_{i}^{o_x}\sum_{a}^{v_y}\mathrm{Tr}[\hat{P}_{xi}\hat{R}'\hat{P}_{ya}\hat{X}], \quad (40)$$

$$\Delta E_{x\rightarrow y}^{\mathrm{RS}}=\sum_{i}^{o_x}\sum_{a}^{v_y}\mathrm{Tr}[\hat{P}_{xi}\hat{F}\hat{P}_{ya}\hat{X}]. \quad (41)$$

Properties (34) and (35) ensure that the charge and energy components sum up to the correct total values:

$$\Delta Q_{\mathrm{CT}}^{\mathrm{RS}}=\sum_{x,y}\Delta Q_{x\rightarrow y}^{\mathrm{RS}}=\sum_{xi}^{O}\sum_{ya}^{V}\Delta Q_{xi\rightarrow ya}^{\mathrm{RS}}, \quad (42)$$

$$\Delta E_{\mathrm{CT}}^{\mathrm{RS}}=\sum_{x,y}\Delta E_{x\rightarrow y}^{\mathrm{RS}}=\sum_{xi}^{O}\sum_{ya}^{V}\Delta E_{xi\rightarrow ya}^{\mathrm{RS}}. \quad (43)$$

Downloaded 26 Nov 2008 to 128.32.49.120. Redistribution subject to AIP license or copyright; see http://jcp.aip.org/jcp/copyright.jsp

It should be noted that $\Delta Q_{\mathrm{CT}}^{\mathrm{RS}}$ and $\Delta E_{\mathrm{CT}}^{\mathrm{RS}}$ do not depend on the choice of partition operators ($\hat{P}_{xq}$). Their values are defined by the natural and unambiguous partitioning of the Hilbert space into occupied ($\hat{R}$) and unoccupied ($\hat{Q}$) subspaces. However, when one attempts to define forward and backbonding components of these terms, it is impossible to avoid ambiguities associated with the partitioning of the occupied and virtual spaces into molecular (or orbital) subspaces. In other words, there is no unique definition for operators $\hat{P}_{xq}$. This problem is closely related to the problem of describing charge distribution among nonorthogonal subspaces associated with orbitals, atoms, or molecules in PA methods. The most widely used partition operators in PA are Mulliken and Löwdin operators.[34–36,54] Mulliken partition operators are not Hermitian which sometimes leads to unphysical negative orbital populations and the population of some orbitals being higher than two. It can be shown, however, that the deviations from the physical [0, 2] interval are second order in the overlap between the orbitals.[40] Such deviations can be considered acceptable in many applications especially for partitioning electron density in molecular complexes since overlap effects between molecules in such complexes are generally smaller than, for example, overlap between atoms in molecules. Orbital populations obtained from the Löwdin partitioning are always within the physical interval but the basis set functions cannot be made strictly localized in this approach.

A Mulliken-type partitioning defined by the following equations:

$$\hat{P}_{xi} = |\psi_{xi}\rangle\langle\psi^{\bar{x}i}|, \tag{44}$$

$$\hat{P}_{xa} = |\tilde{\psi}_{xa}\rangle\langle\tilde{\psi}^{\bar{x}a}| \tag{45}$$

is the best choice for the ALMO decomposition analysis since (i) the polarized reference gives zero intermolecular charge transfer according to the Mulliken PA and (ii) the charge transfer energy terms within a molecule, $\Delta E_{x\to x}^{\mathrm{RS}}$, are zero if the Mulliken-type partitioning is used because the variational optimization of ALMOs nullifies intramolecular occupied-virtual elements of the contravariant-covariant matrix of the Fock operator $\langle\psi^{\bar{x}i}|\hat{F}|\tilde{\psi}_{xa}\rangle$ [see Eq. (47) below]. Matrix equations for intermolecular charge transfer components and their energy on the basis of the polarized ALMOs with the Mulliken-type partitioning are as follows:

$$\Delta Q_{x\to y}^{\mathrm{RS}} = \sum_{i}^{o_x}\sum_{a}^{v_y}\langle\psi^{\bar{x}i}|\hat{R}'|\tilde{\psi}_{ya}\rangle\langle\tilde{\psi}^{\bar{y}a}|\hat{X}|\psi_{xi}\rangle = \mathrm{Tr}[\mathbf{R}'_{(xy)}\mathbf{X}_{(yx)}], \tag{46}$$

$$\Delta E_{x\to y}^{\mathrm{RS}} = \sum_{i}^{o_x}\sum_{a}^{v_y}\langle\psi^{\bar{x}i}|\hat{F}|\tilde{\psi}_{ya}\rangle\langle\tilde{\psi}^{\bar{y}a}|\hat{X}|\psi_{xi}\rangle = \mathrm{Tr}[\mathbf{F}_{(xy)}\mathbf{X}_{(yx)}], \tag{47}$$

where $\mathbf{R}'_{(xy)}$ and $\mathbf{F}_{(xy)}$ are $o_x\times v_y$ matrices and $\mathbf{X}_{(yx)}$ is a $v_y\times o_x$ matrix.

The same partitioning of the charge transfer energy term is used in the ALMO EDA.[26] Our tests show that the Löwdin-type partitioning (i.e., symmetric orthogonalization of the occupied and projected virtual orbitals) produces results that are close to the Mulliken-type analysis. However, intrafragment components are slightly larger in the Löwdin-type approach due to partial delocalization of ALMOs after symmetric orthogonalization.

D. Significant complementary occupied-virtual pairs

Equations (46) and (47) clearly show that in the canonical polarized ALMO, basis charge transfer from molecule x to molecule y is represented as *each* occupied orbital on x donating electrons to *each* virtual orbital on y. In general, there are no occupied-virtual pairs in this representation that can be neglected. However, orbital rotations within the occupied subset and the virtual subset of a molecule leave $\Delta Q_{x\to y}^{\mathrm{RS}}$ and $\Delta E_{x\to y}^{\mathrm{RS}}$ unchanged. Thus, we can use this freedom to find such unitary matrices $\mathbf{U}_x^{(o)}$ and $\mathbf{U}_x^{(v)}$ that rotate orbitals within the occupied subset of molecule x and the virtual subset of molecule y, respectively, to perform singular value decomposition of $\mathbf{X}_{(yx)}$:

$$\mathbf{X}_{(yx)} = \mathbf{U}_y^{(v)}\mathbf{x}_{(yx)}\mathbf{U}_x^{(o)\dagger}, \tag{48}$$

where the $v_y\times o_x$ matrix $\mathbf{x}_{(yx)}$ contains $\min(v_y,o_x)$ singular values of $\mathbf{X}_{(yx)}$ on the diagonal and zeros off the diagonal. Because of the diagonal structure of $\mathbf{x}_{(yx)}$, in the new representation, charge transfer from x to y is described as each occupied orbital on x donating electrons to only *one* (complementary) virtual orbital on y. If $o_x>v_y$, then (o_x-v_y) occupied orbitals on x will not participate in the intermolecular bonding between x and y at all:

$$\begin{aligned}\Delta Q_{x\to y}^{\mathrm{RS}} &= \mathrm{Tr}[(\mathbf{U}_x^{(o)\dagger}\mathbf{R}'_{(xy)}\mathbf{U}_y^{(v)})(\mathbf{U}_y^{(v)\dagger}\mathbf{X}_{(yx)}\mathbf{U}_x^{(o)})]\\ &= \mathrm{Tr}[\mathbf{r}'_{(xy)}\mathbf{x}_{(yx)}],\end{aligned} \tag{49}$$

$$\begin{aligned}\Delta E_{x\to y}^{\mathrm{RS}} &= \mathrm{Tr}[(\mathbf{U}_x^{(o)\dagger}\mathbf{F}_{(xy)}\mathbf{U}_y^{(v)})(\mathbf{U}_y^{(v)\dagger}\mathbf{X}_{(yx)}\mathbf{U}_x^{(o)})]\\ &= \mathrm{Tr}[\mathbf{f}_{(xy)}\mathbf{x}_{(yx)}].\end{aligned} \tag{50}$$

Orbitals constructed by performing unitary transformations $\mathbf{U}_x^{(o)}$ within the occupied subset of molecule x and $\mathbf{U}_y^{(v)}$ within the virtual subset of molecule y are called complementary occupied-virtual pairs (COVPs) for the $x\to y$ intreaction. Construction of the COVPs greatly simplifies the picture of intermolecular orbital interactions. A set of all complementary occupied-virtual pairs describes charge transfer between a pair of molecules *exactly*. We will show in Sec. III that the major contribution to bonding between two molecules (in terms of both energy and amount of electrons transferred) comes from just a few (one or two) COVPs, which we will call significant complementary occupied-virtual pairs. Such pairs provide approximate simplified representation of intermolecular orbital interactions which is useful for a conceptual description of intermolecular bonding.

E. Counterpoise correction

The basis set superposition error (BSSE) is not introduced when the absolutely localized MOs are used to calculate the intermediate state $\hat{R}_{\mathrm{POL}}$ because the constrained MO

Downloaded 26 Nov 2008 to 128.32.49.120. Redistribution subject to AIP license or copyright; see http://jcp.aip.org/jcp/copyright.jsp

optimization prevents electrons on one molecule from borrowing the AOs of other molecules to compensate for incompleteness of their own AOs. However, the BSSE enters the charge transfer contribution since both the BSSE and charge transfer result from the same physical phenomenon of delocalization of fragment MOs. All charge transfer terms reported in this work (ΔE_{CT}, ΔQ_{CT}, and their components) are counterpoise corrected.

The charge transfer obtained from the fully converged SCF calculations are corrected using the standard counterpoise correction method of Boys and Bernardi.[55] In this method, full SCF calculations are performed for each molecule with the ghost orbitals in place of all orbitals of the other molecules. All charge transfer terms calculated with the single RS method are BSSE corrected using similar single RS counterpoise calculations. In this modification of the original Boys–Bernardi method, calculations are also performed separately for each molecule and the ghost orbitals also replace orbitals on the rest of the molecules. However, instead of full SCF calculations, only one RS is performed by solving the amplitude equation [Eq. (30)] starting from the fully converged orbitals of the isolated molecule with no ghost orbitals.

The difference between the Roothaan step counterpoise correction, $\Delta E_{\mathrm{BSSE}}^{\mathrm{RS}}$ ($\Delta Q_{\mathrm{BSSE}}^{\mathrm{RS}}$), and the variational (Boys–Bernardi) correction, ΔE_{BSSE} (ΔQ_{BSSE}), can be treated as higher order BSSE and is generally very small (see Sec. III).

III. RESULTS AND DISCUSSION

The ALMO CTA and ALMO EDA algorithms were implemented in the Q-CHEM software package.[56] We also implemented the Dapprich–Frenking CDA and PA methods to compare them to the ALMO decomposition analysis. We verified that our implementation of CDA reproduces literature results.[48] Charge transfer terms for the Mulliken PA and CDA are calculated according to Eqs. (A9) and (A12), respectively. All charge transfer terms presented in this paper are BSSE corrected. The BSSE is presented in the tables just to show the degree of the basis set completeness.

When $\Delta Q_{\mathrm{CT}}^{\mathrm{RS}}$ is partitioned into pairwise molecule-to-molecule contributions, small spurious negative intramolecular, $\Delta Q_{x\to x}$, terms are often observed. Such negative terms arise from overlap effects and are common in all methods that use Mulliken-type (biorthogonal basis) treatment of the orbital overlap and disappear if Löwdin-type (symmetric orthogonalization) partitioning is used. These negative intrafragment transfer terms can, in principle, be removed by excluding intramolecular excitation terms from the $\hat{X}$ operator when solving Eq. (30). However, the spurious terms are usually significantly smaller that the dominant intermolecular terms and do not complicate the analysis. In order to keep the theory simple, we did not attempt to remove them in this work.

A. Simple two-orbital system: Minimal basis H_2

Before using ALMO CTA on real chemical systems, we would like to apply it to a simple system of two closed shell ions H^- (fragment A) and H^+ (fragment B) that interact with each other to form a closed shell molecule, H_2. This example will help us to illustrate several important concepts and to clarify the difference between the PA methods and ALMO CTA. For the sake of simplicity, we consider a restricted minimal basis set case, so each fragment in the system has only one molecular orbital. The process of the H_2 molecule formation can be represented by three states schematically shown in Fig. 1.

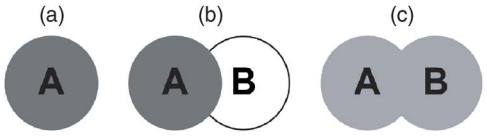

FIG. 1. (Color online) A simple system of two subsystems.

(1) In the initial state of infinitely separated ions, the orbital on H^-, $|\psi_A\rangle$, is doubly populated and the orbital on H^+, $|\psi_B\rangle$, is empty [Fig. 1(a)].
(2) In the intermediate state, the ions are brought to their equilibrium geometry in the H_2 molecule but their densities are not allowed to relax [Fig. 1(b)]. The molecular orbital overlap in this state is $\sigma_{AB}=\langle\psi_A|\psi_B\rangle$.
(3) In the final state, $\hat{R}_{\mathrm{SCF}}$, the density is relaxed to self-consistency [Fig. 1(c)].

Our main goal is to quantify the amount of charge transfer when the molecule is formed. To make this example more illustrative, we compare ions *A* and *B* to two cities A and B. Figure 1 may then be regarded as showing three population snapshots in the history of the cities:

(1) City A is populated and city B is not built yet [Fig. 1(a)].
(2) City B is built in the close proximity of A [Fig. 1(b)] but the new houses are still empty.
(3) People moved from city A to new houses in city B, and the final population density is uniform [Fig. 1(c)].

In this analogy, finding the degree of charge transfer is equivalent to answering the question "How many people moved after city B was built?." The answer to the demographic question is relatively simple: All people who live in the new houses did move (it is, of course, assumed that people who are still in A did not move from one apartment to another). Mathematically, the answer is the integral of the final population density over the white area in Fig. 1(b). Note that it would be incorrect to integrate over the area of city B in an attempt of finding the answer (in fact, we do not even have to define the area of city B yet).

Therefore, to find the amount of electron transfer ΔQ, it is necessary to integrate the final electron distribution $\hat{R}_{\mathrm{SCF}}$, over the previously "unoccupied" Hilbert subspace which is spanned by the *projected* orbital B, $|\tilde{\psi}_B\rangle$:

$$|\tilde{\psi}_B\rangle=(\hat{1}-\hat{R})|\psi_B\rangle=\frac{1}{\sqrt{1-\sigma_{AB}^2}}(|\psi_B\rangle-|\psi_A\rangle\sigma_{AB}), \tag{51}$$

Downloaded 26 Nov 2008 to 128.32.49.120. Redistribution subject to AIP license or copyright; see http://jcp.aip.org/jcp/copyright.jsp

TABLE I. B3LYP ALMO CTA and EDA results for borane complexes. Geometry is optimized at B3LYP/6-31(+,+)G(d,p) level. Basis sets used for ALMO analysis are (1) 6-31G, (2) 6-31G(d,p), (3) 6-31(+,+)G(d,p), (4) 6-31(+,+)G(df,pd), and (5) 6-31(2+,2+)G(df,pd). All terms are BSSE corrected.

	H_3B-CO										H_3B-NH_3									
Scale	ΔQ (m$\bar{e}$)					ΔE (kJ/mol)					ΔQ (m$\bar{e}$)					ΔE (kJ/mol)				
Basis	1	2	3	4	5	1	2	3	4	5	1	2	3	4	5	1	2	3	4	5
FRZ			0			232	274	317	313	315			0			−5	45	103	106	106
POL			0			−127	−164	−203	−222	−227			0			−67	−89	−128	−132	−133
RS(D→D)[a]	−3	−5	−7	−7	−8			0			−5	−8	−5	−5	−2			0		
RS(D→BH_3)[a]	46	45	46	40	41	−140	−145	−143	−126	−123	55	58	58	26	53	−113	−124	−134	−131	−130
RS(BH_3→D)[a]	196	173	180	178	178	−132	−128	−131	−129	−128	5	5	8	8	8	−6	−9	−11	−11	−11
RS(BH_3→BH_3)	−5	−4	−5	−8	−8			0			−1	−1	−1	−1	−2			0		
HO-CT	−21	−15	−20	−22	−22	−9	−11	−8	−6	−6	−1	0	2	2	2	0	−2	−3	−3	−3
TOTAL	**213**	**195**	**195**	**182**	**181**	**−177**	**−173**	**−168**	**−170**	**−170**	**53**	**54**	**61**	**59**	**59**	**−190**	**−178**	**−172**	**−172**	**−172**
BSSE	7	5	1	1	1	15	11	3	5	5	10	9	3	3	3	16	13	6	7	6
RS-BSSE	6	4	1	1	1	14	10	3	5	5	8	7	3	3	3	15	12	6	7	6
MPA TOTAL	739	835	1005	1019	1000			N/A			319	374	543	559	435			N/A		
MPA $Q(BH_3)$	53	−90	−324	−283	−416						−243	−299	−538	−551	−743					

[a]D stands for CO in BH_3-CO and for NH_3 in BH_3-NH_3.

$$\Delta Q = \langle \tilde{\psi}_B | \hat{R}_{SCF} | \tilde{\psi}_B \rangle = 1 - \sigma_{AB}. \tag{52}$$

Equation (52) is exactly our main working equation [Eq. (14)] applied to a two-orbital system with one occupied and one virtual orbital. For the H_2 molecule with the interatomic distance 0.700 Å and with the STO-3G basis set functions on the atoms (σ_{AB}=0.686), the charge reorganization from the intermediate state to the final state is 0.314$\bar{e}$. There is no electron reorganization going from the initial to the intermediate state since the electron densities are kept fixed.

In a PA, one determines the amount of electron density that "belongs" to each hydrogen atom in the final state. To do this, it is necessary to specify how the Hilbert space is partioned among the overlaping reference atomic orbitals. This problem is similar to finding the final population of each city in Fig. 1(c) and requires integration over the *area* of the city. In Mulliken PA, population of orbitals are calculated as diagonal elements of the density matrix in the "natural" contravariant-covariant (or biorthogonal) representation. In the H_2 case, the initial and the final population of orbital B are 0$\bar{e}$ and 1$\bar{e}$, respectively:

$$pop_B(R_{FRZ}) = \langle \psi^B | \hat{R}_{FRZ} | \psi_B \rangle = 0, \tag{53}$$

$$pop_B(R_{SCF}) = \langle \psi^B | \hat{R}_{SCF} | \psi_B \rangle = 1, \tag{54}$$

$$|\psi^B\rangle = \frac{1}{1-\sigma_{AB}^2}(|\psi_B\rangle - |\psi_A\rangle\sigma_{AB}), \tag{55}$$

$$\Delta Q^{(MPA)} = pop_B(R_{SCF}) - pop_B(R_{FRZ}) = 1. \tag{56}$$

Therefore, it is said that the formal charges on atoms in the H_2 molecule are zero and that one electron is transferred from H^- to H^+ when the H_2 molecule is formed [see Eq. (A9) in Appendix].

In PA, electron transfer effects are inferred from integrating over the orbital $|\psi_B\rangle$ not over the unoccupied subspace defined by projected orbital orbital $|\tilde{\psi}_B\rangle$. This is the main reason for the difference between the CTA and PA results. This difference is not surprising since these two methods are designed to solve different problems (transfer versus population). CTA measures charge transfer effects with well defined energies, while PA values for charge transfer are consistent with the formal charges on atoms. A detailed comparison of ALMO CTA and PA is presented in the Appendix.

B. Donor-acceptor interactions in H_3B-CO and H_3B-NH_3

Donor-acceptor bonding is a central concept in chemistry.[57–59] Borane compounds such as ammonia borane (H_3B-NH_3) and borane carbonyl (H_3B-CO) are textbook examples of donor-acceptor complexes. Donor-acceptor bonding in these compounds has been the subject of numerous experimental[60,61] and theoretical studies.[19,25,48,62–66] ALMO energy decomposition analysis[25,26,66] as well as application of other EDA methods[19,63] have shown that the electronic structure of ammonia borane is correctly described by a simple Lewis structure with the nitrogen atom donating its lone electron pair into the empty orbital of the boron atom. The donor-acceptor bonding in borane carbonyl has more complicated character with significant contribution of back-donation of the electron density from BH_3 to CO.[26,48,63,65]

The standard Kohn–Sham DFT with the B3LYP functional and 6-31(+,+)G(d,p) basis set was used to obtain the complex geometries. Decomposition analysis was performed using the same functional for a series of five basis sets from the 6-31G family with increasing number of polarized and diffuse functions on atoms (Table I). The ALMO decomposition method demonstrates very good stability: Both energy and charge components change only slightly as the basis set size increases. As shown before,[26] the total interaction energies are approximately the same for H_3B-NH_3 and H_3B-CO but the fundamental nature of donor-acceptor interactions is very different (Table I). While H_3B-NH_3 is better stabilized by noncharge transfer interaction (ΔE_{FRZ}

Downloaded 26 Nov 2008 to 128.32.49.120. Redistribution subject to AIP license or copyright; see http://jcp.aip.org/jcp/copyright.jsp

TABLE II. Dapprich–Frenking CDA for borane complexes. Geometry is optimized at B3LYP/6-31(+,+)G(d,p) level. Basis sets used for CDA analysis are (1) 6-31G, (2) 6-31G(d,p), (3) 6-31(+,+)G(d,p), (4) 6-31(+,+)G(df,pd), and (5) 6-31(2+,2+)G(df,pd). All terms are in m$\bar{e}$ and are not BSSE corrected.

Scale	H_3B-CO				H_3B-NH_3			
Basis	1	2	3	4	1	2	3	4
$2^*\Delta Q(\mathrm{occ(D)}\rightarrow\mathrm{vir}(BH_3))$[a]	537	538	458	432	345	411	383	376
$2^*\Delta Q(\mathrm{occ}(BH_3)\rightarrow\mathrm{vir(D)})$[a]	301	340	342	300	−4	31	−97	−154
$2^*\Delta Q(\mathrm{occ(D)}\rightarrow\mathrm{occ}(BH_3))$[a]	−349	−218	−381	−437	−417	−328	−642	−688
$2^*\Delta Q(\mathrm{vir(D)}\rightarrow\mathrm{vir}(BH_3))$[a]	−4	−3	−34	−31	−4	−13	−50	−61
$\Delta Q(\mathrm{vir(D)}\rightarrow\mathrm{vir(D)})$[a]	201	194	202	207	15	19	55	63
$\Delta Q(\mathrm{vir}(BH_3)\rightarrow\mathrm{vir}(BH_3))$	280	357	348	324	136	186	188	191

[a]D stands for CO in BH_3-CO and for NH_3 in BH_3-NH_3.

and ΔE_{POL}) than H_3B-CO, the charge transfer effects in the latter are stronger due to backdonation from H_3B to CO.

$\Delta Q_{\mathrm{CT}}^{\mathrm{RS}}$ terms (Table I) show no evidence of significant backdonation in H_3B-NH_3, which is in excellent agreement with the energy terms. The electronic structure of this complex is well described by the single RS—the higher order relaxation terms are very small. By contrast, the backdonation term in H_3B-CO is stronger than forward donation and the occupied-virtual mixing is accompanied by strong induction (i.e., $\Delta Q_{\mathrm{CT}}^{\mathrm{HO}}$ is not negligible).

It is remarkable that the ratio of the backbonding and forward donation terms in borane carbonyl is significantly different on the charge and energy scales ($\Delta Q_{\mathrm{back}}/\Delta Q_{\mathrm{forw}} \approx 4$, whereas $\Delta E_{\mathrm{back}}/\Delta E_{\mathrm{forw}} \approx 1$). In the perturbation theory, which describes the charge transfer correction to the zero-order polarized state [Eqs. (46) and (47)], ΔQ terms are proportional to the product of the single excitation amplitudes with the density matrix elements ($\Delta Q \propto R'_{ia}X_{ai}$), whereas ΔE terms are proportional to the product of the amplitudes with the Fock matrix elements ($\Delta E \propto F_{ia}X_{ai}$). Therefore, the ratio of the relative strength of forward and backward charge transfer on the charge and energy scale is determined by the ratio of the corresponding Fock and density matrix elements:

$$\frac{\Delta Q_{\mathrm{back}}/\Delta Q_{\mathrm{forw}}}{\Delta E_{\mathrm{back}}/\Delta E_{\mathrm{forw}}} \propto \frac{F_{\mathrm{forw}}}{F_{\mathrm{back}}}\frac{R'_{\mathrm{back}}}{R'_{\mathrm{forw}}}. \tag{57}$$

For H_3B-CO, the ratios of the matrix elements corresponding to the most significant charge transfer terms (see COVPs below) are $F_{\mathrm{forw}}/F_{\mathrm{back}} \approx 2$ and $R'_{\mathrm{back}}/R'_{\mathrm{forw}} \approx 2$. This example illustrates the value of the charge scale introduced in this work and shows that π-bonding (backdonation) in borane carbonyl is approximately four times weaker than σ-bonding (forward donation) if measured in terms of energy/per electron transferred.

The absolute values of ΔQ show that intermolecular charge transfer effects are significantly smaller than those inferred from the Mulliken population analysis (Table I). The ALMO CTA intermolecular electron transfer does not exceed $0.06\bar{e}$ in H_3B-NH_3 and $0.20\bar{e}$ in H_3B-CO, whereas MPA predicts transfer of approximately $0.50\bar{e}$ in H_3B-NH_3 and $1.00\bar{e}$ in H_3B-CO. Moreover, MPA predicts that the BH_3 fragment is negatively charged, in disagreement with ALMO CTA which gives stronger donation from BH_3. As shown in the Appendix, the major difference between ALMO CTA and MPA is in the treatment of virtual orbitals. ALMO CTA uses *projected* virtual orbitals to ensure that all measured charge transfer effects are only due to relaxation of the localized occupied orbitals into the virtual subspace. Such delocalization has a well defined energy since ΔE can be assigned only to charge transfer to the strongly orthogonal virtual subspace. In PA methods, which are originally constructed to measure formal charges on the fragments, virtual orbitals are treated on the same footing with occupied orbitals. Therefore, formal charges and ΔQ inferred from PA methods include both the effect of relaxation of the occupied orbitals (i.e., true delocalization) as well as the effect of occupied-virtual overlap (see the H_2 example above and the Appendix for a detailed comparison of these two methods). It is also not uncommon for MPA to predict charges of the wrong sign even in very simple systems.[67]

Of course, construction of the projected virtual orbitals in ALMO methods unavoidably destroys absolute locality of the virtual orbitals [Eq. (11)]. We verified, however, that the degree of such a delocalization is not significant. Moreover, ALMO CTA calculations with very compact STO-3G basis set reproduce the results presented in Table I. Therefore, all charge transfer terms in ALMO CTA have properly localized donor and acceptor centers. We conclude that despite the common view on the bonding in borane carbonyl, CO is a better Lewis acid than BH_3.

We also performed the CDA proposed by Dapprich and Frenking.[48] CDA is based on the same principles as MPA and, therefore, also produces large charge transfer terms (Table II). As demonstrated in the Appendix, some of the CDA terms do not have clear physical meaning. For example, intramolecular virtual-virtual terms do not correspond to any physical effect and can be of the same order of magnitude as the forward donation and backbonding terms (Table II).

It is interesting to note that small charge transfer terms (i.e., similar to ALMO CTA) are obtained for H_3B-NH_3 in the work of Mo and Gao.[68] To calculate the amount of electron density transferred from NH_3 to BH_3, these authors applied natural population analysis to the polarized reference and to the fully relaxed wavefunction and took the difference of the charges on NH_3. In this approach the polarized refer-

Downloaded 26 Nov 2008 to 128.32.49.120. Redistribution subject to AIP license or copyright; see http://jcp.aip.org/jcp/copyright.jsp

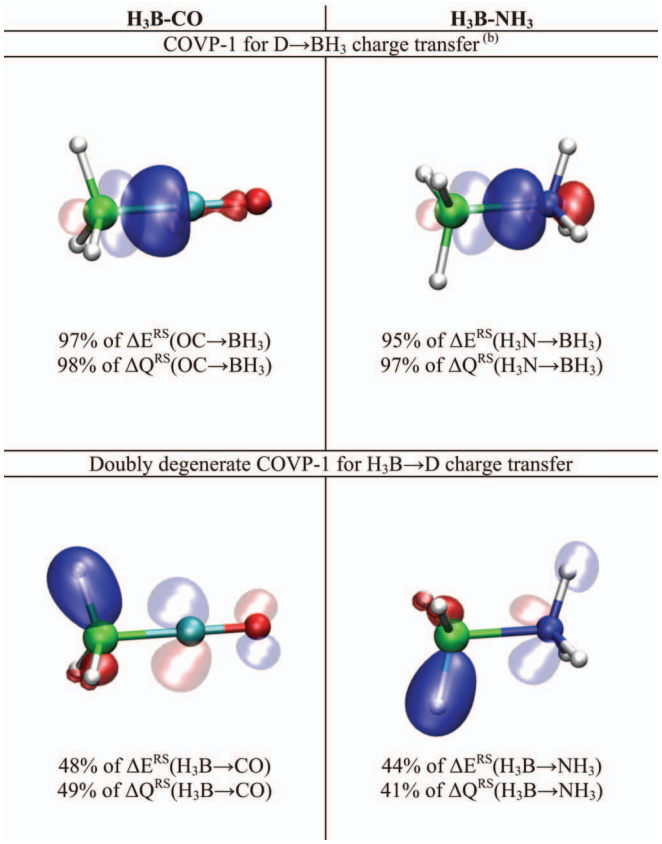

FIG. 2. (Color) Significant COVPs in borane complexes calculated at the B3LYP/6-31(+,+)G(d,p) level. Isovalue surface of 0.15 a.u. Occupied orbitals are represented with saturated colors. Faint colors represent complementary virtual orbitals. D stands for CO in BH_3-CO and for NH_3 in BH_3-NH_3.

ence state also plays the key role but this method incorrectly produces nonzero charge transfer for the polarized state. It would also fail to separate ΔQ into forward and backdonation components for systems in which both effects are important (e.g., H_3B-CO).

Absolutely localized complementary occupied-virtual pairs for borane complexes at the equilibrium geometry were constructed at the B3LYP/6-31(+,+)G(d,p) level of theory. The most significant orbitals for forward donation and backbonding are shown in Fig. 2. In agreement with the classical donor-acceptor theory, the donating occupied orbitals on NH_3 and CO fragments closely resemble sp^3-hybridized lone pairs while the virtual orbitals are sp^3-hybridized empty orbitals on the boron atom. These pairs recover more than 95% of the overall charge transfer in this direction. The backbonding complementary orbital pairs in H_3B-CO are doubly degenerate and each recover 48%–49% of backdonation (only one of the two degenerate orbitals is shown in Fig. 2). Figure 2 indicates that backdonation occurs from the B–H σ-bonding orbitals to the antibonding π^* orbital of the CO molecule.

C. Bonding in carbonyl complexes

The CO ligand is one of the most important ligands in chemistry of transition metals. The metal-carbonyl bonding is a classic example of the Dewar–Chatt–Duncanson model of synergic bonding in metal complexes.[50,51] According to this model, the carbonyl ligand donates an electron pair from the occupied antibonding orbital on the carbon atom (so-called 5σ orbital) into the metal unoccupied orbitals, and the metal donates the electron density back from its occupied orbitals into the carbonyl π^*-antibonding orbitals.[69,70] As a result of the metal-ligand interaction, metal-carbonyl complexes exhibit C–O stretching frequencies that are shifted from the frequency of the free CO molecule. In "classical" carbonyl complexes, the C–O stretching frequency is lower than in isolated CO. This shift is interpreted as a result of strong backdonation into the antibonding π^* orbitals of the CO molecule which weakens the C–O bond.[70] In another class of metal-carbonyl complexes, called "nonclassical" carbonyls, the C–O stretching mode is close to or even higher in energy than that in free CO.[71–74] This unusual behavior is attributed to donation from the CO antibonding 5σ orbital without compensating backdonation into the CO antibonding π^* orbitals.[48,71,73,74]

The relative strength of forward donation and backbonding effects in metal-carbonyl complexes can be made quantitative with ALMO CTA. In this work, we applied ALMO decomposition to typical nonclassical complexes-$AgCO^+$ and $AuCO^+$, and to a classical carbonyl-$W(CO)_6$. Complex geometries were optimized using the B3LYP density functional with the effective core potential LANL2DZ basis for the metal atoms and the 6-31+G(d) basis for all other atoms. The EDA calculations are also done at the B3LYP/LANL2DZ/6-31+G(d) level and the results are summarized in Table III.

As evident from the computed bond lengths and vibrational frequencies (Table III), the C–O bond, indeed, becomes shorter and stronger in nonclassical carbonyls, $AgCO^+$ and $AuCO^+$. The opposite trend is observed for classical $W(CO)_6$. In agreement with the widely accepted understanding of bonding in carbonyls, the backbonding charge transfer energy components are smaller relative to the forward donation terms in nonclassical carbonyls, whereas $\Delta E^{RS}_{M\rightarrow CO}$ in the classical carbonyl is noticeably larger than $\Delta E^{RS}_{CO\rightarrow M}$.

The same trends are observed on the charge scale. The only exception is that forward- and backdonation terms on the charge scale in $AuCO^+$ are of the same magnitude, while forward donation is twice as large as backdonation on the energy scale (for explanations, see the H_3B-CO example above). To verify that our method properly separates forward-donation and backbonding terms in $AuCO^+$ we applied ALMO CTA to AuCN and compared results for these two complexes (Table III). CO is known as a strong, well balanced σ-donor and π-acceptor, while the CN^- ligand is a good σ-donor and very poor π-acceptor. ALMO CTA correctly predicts large forward-donation and negligible backbonding for AuCN.

Based on the results of ALMO CTA and ALMO EDA, we conclude that backbonding in nonclassical carbonyls is not negligible even though this effect is smaller than forward donation. Backdonation to the CO virtual antibonding orbitals does not fully compensate for forward donation from the occupied CO orbitals in nonclassical carbonyls. The back-

Downloaded 26 Nov 2008 to 128.32.49.120. Redistribution subject to AIP license or copyright; see http://jcp.aip.org/jcp/copyright.jsp

TABLE III. ALMO CTA and EDA results for carbonyl complexes. Geometry optimization and decomposition analysis are performed at B3LYP/LANL2DZ/6-31+G(d) level. All terms are BSSE corrected.

	Ag^+-CO		Au^+-CO		$(CO)_5W-CO$		Au^+-CN^-	
Scale	ΔQ (m$\bar{e}$)	ΔE (kJ/mol)	ΔQ (m$\bar{e}$)	ΔE (kJ/mol)	ΔQ (m$\bar{e}$)	ΔE (kJ/mol)	ΔQ (m$\bar{e}$)	ΔE (kJ/mol)
frz	0.0	22.0	0.0	180.3	0.0	138.4	0.0	−388.4
pol	0.0	−60.8	0.0	−159.1	0.0	−68.7	0.0	−205.4
RS(M→M)	−0.4	0.0	5.3	0.0	−2.8	0.0	14.0	0.0
RS(M→L)[a]	12.0	−14.1	55.5	−66.9	245.9	−141.7	16.7	−31.2
RS(L→M)[a]	27.8	−37.0	58.9	−132.8	37.3	−101.0	205.7	−259.3
RS(L→L)[a]	−12.9	0.0	−6.5	0.0	8.2	0.0	−46.7	0.0
HO-CT	5.9	−3.1	33.5	−17.2	−27.7	−11.8	−5.9	−0.8
TOTAL	**32.3**	**−93.1**	**146.8**	**−195.8**	**260.9**	**−184.8**	**183.6**	**−885.2**
BSSE	0.9	1.9	0.8	2.4	2.2	6.6	1.1	2.6
RS-BSSE	0.8	1.8	0.7	2.3	2.0	6.4	1.0	2.5
d(C−O/N) (Å)[b]	1.126		1.126		1.151		1.166	
υ(C−O/N) (cm^{-1})[b]	2305		2302		2056		2273	

[a]L stands for CO in the carbonyl complexes and for CN^- in the Au^+-CN^- complex.
[b]d(C−O)=1.137 Å and υ(C−O)=2203 cm^{-1} in the uncoordinated CO molecule. d(C−N)=1.183 Å and υ(C−N)=2125 cm^{-1} in the uncoordinated CN^- anion.

bonding term in the classical tungsten carbonyl is significantly stronger that the forward donation term. The relative strength of these terms explain blue and red shifts in vibrational spectra of coordinated CO in nonclassical and classical carbonyls.[74]

This explanation is supported by the more detailed COVP analysis which shows that in both classes of carbonyl complexes almost 100% of forward donation is recovered with a single COVP. The shape of the occupied orbital of this COVP (Fig. 3) is exactly the shape of the HOMO of the CO molecule (5σ orbital). The backdonation to the CO antibonding doubly degenerate π^* orbitals recovers 100% of the transfer in classical carbonyls and 77% in nonclassical carbonyls. The remaining 23% of backdonation in nonclassical complexes is due to the transfer into the σ^* orbital of CO (Fig. 3).

D. Multiple intermolecular bonds in a complex of isocyanuric acid and melamine

Isocyanuric acid (1,3,5-triazine-2,4,6-trione) and melamine (1,3,5-triazine-2,4,6-triamine) are thought to be a major cause of two outbreaks of pet food-associated renal failure in cats and dogs.[75] Although neither of these chemicals is individually toxic, it is believed that their potency may increase when they are present together.[76] Isocyanuric acid (ICA) and melamine (MA) can form networks of hydrogen bonds, creating a tilelike planar structure through molecular self-assembly.[1] Three hydrogen bonds formed in the planar ICA-MA complex are shown in Fig. 4 (complex 1). We apply ALMO decomposition to isolate electron transfer effects associated with individual hydrogen bonds in the complex. To verify accuracy of the decomposition, we also compare ALMO CTA results for the planar complex and the complex in which ICA and MA molecules lie in perpendicular planes (complex 2) and in which only one hydrogen bond between the interacting molecules is formed.

Geometry optimization and EDA calculations were performed using the B3LYP density functional with the 6-31(+,+)G(d,p) basis set for all atoms in the system. The results are summarized in Table IV.

In the planar complex, charge transfer from MA to ICA is 19.2 m$\bar{e}$ and charge transfer in the opposite direction is 8.0 m$\bar{e}$. The energy lowering corresponding to these delocalization effects is proportional to the amount of charge transfer and are 32.3 kJ/mol and 15.3 kJ/mol, respectively. Intramolecular effects and the higher order relaxation are small. Charge and energy terms in each directions can be further decomposed into molecular orbital contributions. COVP decomposition shows that 93% of $\Delta E^{RS}_{MA\to ICA}$ and 95% of $\Delta Q^{RS}_{MA\to ICA}$ result from electron donation from the nitrogen's lone pair in MA to the N–H σ-antibonding orbital in ICA (Fig. 5). Two COVPs contribute to this effect. Occupied orbitals in these COVPs are different linear combinations of sp^2-hybridized lone pair orbitals on nitrogen atoms in the aromatic ring of MA. Charge transfer in the opposite direction is primarily due to interactions of the lone pairs on oxygen atoms in ICA with N–H σ-antibonding orbitals in MA (Fig. 5). Again, two COVPs, symmetric and antisymmetric (Fig. 5), contribute to this effect. They account for 64% and 71% of $\Delta E^{RS}_{ICA\to MA}$ and $\Delta Q^{RS}_{ICA\to MA}$, respectively. The remaining charge transfer in this direction is covered by the other 31 COVPs, none of which exceeds 12% and 10% of $\Delta E^{RS}_{ICA\to MA}$ and $\Delta Q^{RS}_{ICA\to MA}$, respectively.

The ALMO decomposition results for complex 1 can be compared to the decomposition for complex 2, in which only one hydrogen bond is formed between the interacting fragments. The difference in ΔE_{FRZ} and ΔE_{POL} between complex 1 and complex 2 can be explained by purely electrostatic effects: Oxygen and hygrogen atoms of the peripheral hydrogen bonds have partial charges of the opposite sign and are closer to each other in complex 1. This leads to stronger electrostatic attraction between MA and ICA and also to stronger mutual polarization in complex 1 compared to complex 2. As expected, charge transfer from ICA to MA in complex 2 is negligible and charge transfer in the opposite direction is very close to that in complex 1. COVP decom-

Downloaded 26 Nov 2008 to 128.32.49.120. Redistribution subject to AIP license or copyright; see http://jcp.aip.org/jcp/copyright.jsp

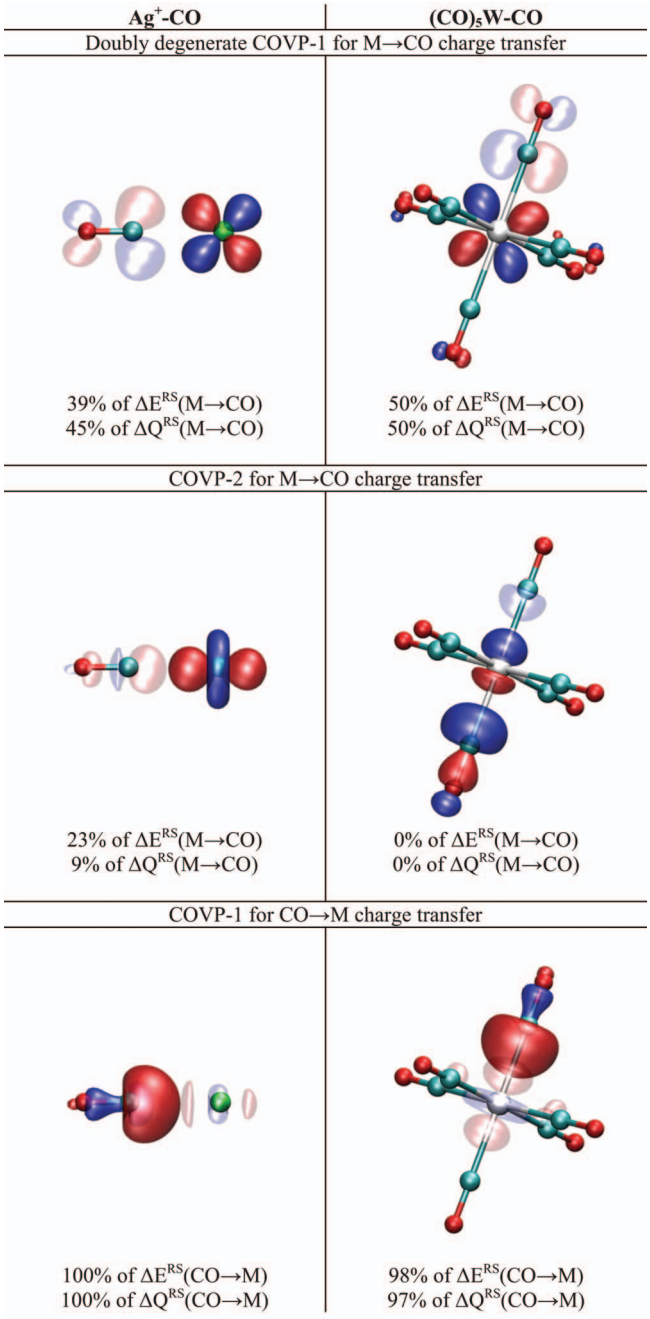

FIG. 3. (Color) Significant COVPs in metal-carbonyl complexes calculated at the B3LYP/LANL2DZ/6-31(+)G(d) level. Isovalue surface of 0.1 a.u. Occupied orbitals are represented with saturated colors. Faint colors represent complementary virtual orbitals.

position for MA→ICA terms in both complexes are almost identical. Small electron transfer effects from ICA to MA in complex 2 do not have dominant terms in the COVP decomposition.

Based on these results we conclude that in the planar complex delocalization effects for the central N···H hydrogen bond is approximately four to five times stronger (19.2 m$\bar{e}$ and 32.3 kJ/mol) than for the peripheral O···H bond (4.0 m$\bar{e}$ and 7.7 kJ/mol).

IV. CONCLUSIONS

Energy decomposition methods based on absolutely localized orbitals (ALMO) have been succesful in studying

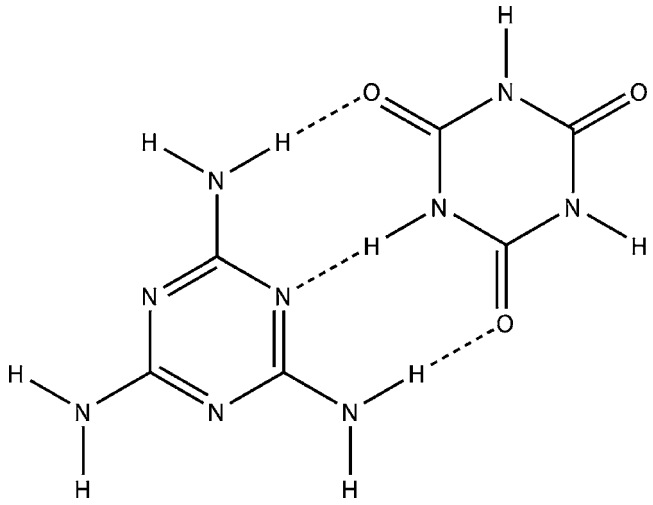

FIG. 4. Complex of isocyanuric acid and melamine (complex 1).

and analyzing binding mechanisms in numerous molecular complexes.[25,26,66–68,77–79] The ALMO energy decomposition analysis (EDA) (Refs. 25 and 26) enables accurate separation of the total intermolecular interaction energy into intramolecular (frozen density and polarization) terms and intermolecular (charge transfer) energy terms.

In this paper, we have extended decomposition analysis method based on absolutely localized molecular orbitals (ALMO). First, we proposed a quantitative scale to measure intermolecular charge transfer effects. All terms on this scale such as forward-donation, backdonation, and higher order relaxation have well defined energetic effects consistent with the previously defined energy terms in ALMO EDA. Second, we introduced concept of chemically significant complementary occupied-virtual orbital pairs which provides a simple description of electron transfer effects in intermolecular interactions.

The newly proposed generalized ALMO decomposition method has been tested successfully on systems involving hydrogen bonding and donor-acceptor interactions. For cases such as borane complexes, metal carbonyls, and complexes with hydrogen bonding ALMO decomposition analysis re-

TABLE IV. ALMO CTA and EDA results for complexes of isocyanuric acid (ICA) with melamine (MA). Geometry optimization and decomposition analysis are performed at B3LYP/6-31(+,+)G(d,p) level. All terms are BSSE corrected.

	Complex 1		Complex 2	
Scale	ΔQ (m$\bar{e}$)	ΔE (kJ/mol)	ΔQ (m$\bar{e}$)	ΔE (kJ/mol)
FRZ	0.0	2.8	0.0	18.8
POL	0.0	−29.2	0.0	−18.2
RS(MA→MA)	−2.5	0.0	−3.1	0.0
RS(MA→ICA)	19.2	−32.3	18.4	−30.0
RS(ICA→MA)	8.0	−15.3	0.4	−1.2
RS(ICA→ICA)	−1.1	0.0	0.1	0.0
HO-CT	3.1	−2.9	1.6	−1.7
TOTAL	**26.8**	**−76.1**	**17.4**	**−32.4**
BSSE	1.1	4.7	1.1	3.3
RS-BSSE	1.1	4.6	1.0	3.2

Downloaded 26 Nov 2008 to 128.32.49.120. Redistribution subject to AIP license or copyright; see http://jcp.aip.org/jcp/copyright.jsp

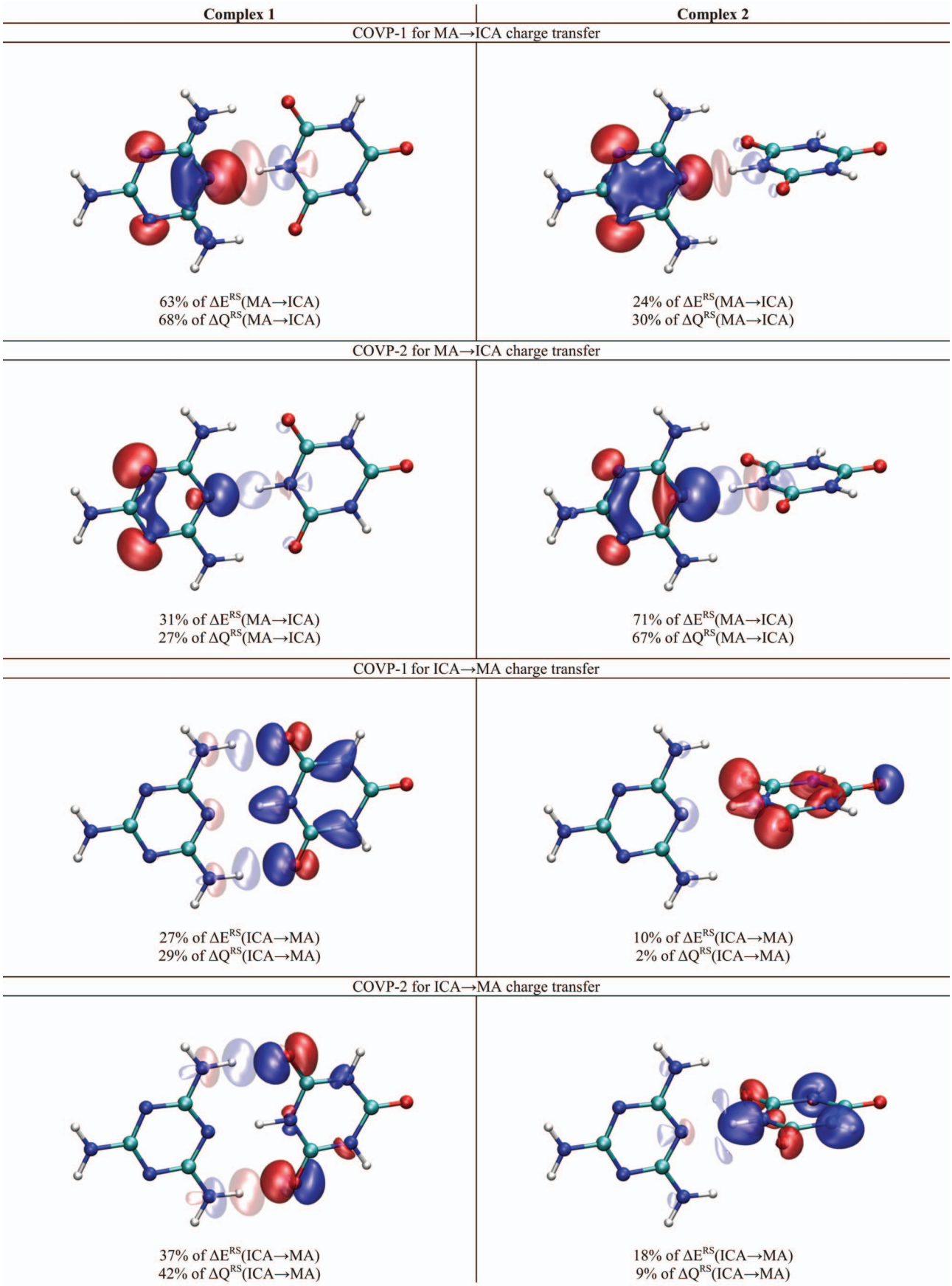

FIG. 5. (Color) Significant COVPs in complexes of isocyanuric acid (ICA) and melamine (MA) calculated at the B3LYP/6-31(+,+)G(d,p) level. Isovalue surface of 0.07 a.u. Occupied orbtials are represented with saturated colors. Faint colors represent complementary virtual orbitals.

Downloaded 26 Nov 2008 to 128.32.49.120. Redistribution subject to AIP license or copyright; see http://jcp.aip.org/jcp/copyright.jsp

sults are broadly consistent with existing understanding of intermolecular bonding. However, according to ALMO charge transfer analysis the amount of electron density transferred between molecules is significantly smaller than charge transfer estimated from various population analysis methods. Additionally, charge transfer and the associated energy lowering are by no means directly proportional to each other, as might sometimes be naively assumed. For example in H_3B-CO, the magnitude of charge backdonated by BH_3 exceeds that forward donated by CO by a factor of approximately four, although forward and back-donation yield similar energy lowering.

ACKNOWLEDGMENTS

This work was supported by the Director, Office of Basic Energy Sciences, Chemical Sciences Division of the U.S. Department of Energy under Contract No. DE-AC03-76SF00098, by the National Science Foundation under Grant No. CHE-0535710, and by BP through the Methane Conversion Cooperative.

APPENDIX:

Comparison of ALMO CTA to population analysis and charge decomposition analysis

As we show in Sec. II, charge transfer effects measured in the ALMO CTA methods are different from charge transfer inferred from the population analysis methods. The major difference between ALMO CTA and population analysis is the way the Hilbert space of the molecular complex is partitioned. The population analysis methods are specifically designed to calculate formal charges on molecules in molecular complexes (see below). In these methods, the entire Hilbert space spanned by nonorthogonal reference orbitals is divided into molecular subspaces with partition operators $\hat{P}_x^{(pa)}$:

$$\hat{P}_x^{(pa)} = \sum_p^{n_x} |\psi_{xp}\rangle\langle\psi^{xp}| \neq (\hat{P}_x^{(pa)})^\dagger. \tag{A1}$$

Although these operators satisfy the idempotency and resolution of identity conditions

$$(\hat{P}_x^{(pa)})^2 = \hat{P}_x^{(pa)}, \tag{A2}$$

$$\sum_x \hat{P}_x^{(pa)} = \hat{1}, \tag{A3}$$

they do not represent true projectors since they are generally non-Hermitian. Therefore, we say that the Hilbert space is *vaguely* partitioned into molecular subspaces in the PA methods.

In contrast, ALMO CTA is constructed to measure the amount of charge reorganization in the final electronic state with respect to some reference state. For the final electronic state, this method calculates the amount of the electron density that occupies the initially unoccupied subspace [see Eq. (14)]. Therefore, ALMO CTA first of all partitions the entire Hilbert space of the reference state into the strongly orthogonal occupied and virtual subspaces with *true* projectors $\hat{R}$ and $\hat{Q}$. Only then, if one is interested in forward donation and backbonding components of the total charge transfer term, both the occupied and virtual subspaces are vaguely partitioned into molecular subspaces with operators $\hat{P}_x^{(o)}$ and $\hat{P}_x^{(v)}$:

$$\hat{P}_x^{(o)} \equiv \sum_i^{o_x} |\psi_{xi}\rangle\langle\psi^{\bar{x}i}| = \sum_i^{o_x} \hat{P}_{xi}, \tag{A4}$$

$$\hat{P}_x^{(v)} \equiv \sum_a^{v_x} |\tilde{\psi}_{xa}\rangle\langle\tilde{\psi}^{\bar{x}a}| = \sum_a^{v_x} \hat{P}_{xa}. \tag{A5}$$

Non-Hermitian idempotent operators $\hat{P}_x^{(o)}$ and $\hat{P}_x^{(v)}$ are not true projectors. In this sense, they are similar to $\hat{P}_x^{(pa)}$. However, they sum up to projectors $\hat{R}$ and $\hat{Q}$ which do define the occupied and virtual subspaces:

$$\sum_x \hat{P}_x^{(o)} = \hat{R}, \tag{A6}$$

$$\sum_x \hat{P}_x^{(v)} = \hat{Q}. \tag{A7}$$

It is important to note that the proper definition of these subspaces allows one to assign the energetic components to charge transfer terms because the corresponding energy lowering is unambiguously defined only for charge transfer from the occupied subspace to the unoccupied subspace [Eq. (21)]. The lack of well defined occupied and unoccupied subspaces in the population analysis makes these methods inapplicable for studying charge transfer. Thus, ALMO CTA gives the correct intermolecular electron transfer and the energy associated with it, whereas PA methods produce the proper formal charges on molecules.

The CDA method[48] attempts to quantify the degree of electron delocalization in molecular complexes. As we show below, CDA uses partitioning operators similar to the Mulliken population analysis operators [Eq. (A1)] and, therefore, suffers from the same shortcomings as the PA methods when it is applied to study electron density relaxation. CDA employs the frozen density state as a reference state, whereas ALMO CTA uses the polarized state. The latter is a more appropriate reference for studying intermolecular electron density transfer since the results are not contaminated by intramolecular relaxation effects. Another serious drawback of CDA is that some terms obtained in this method do not have clear physical interpretation.

A detailed mathematical description of the PA methods and CDA is presented below.

Population analysis

Any one-electron density operator $\hat{R}_f$ (usually constructed from delocalized occupied molecular orbitals) can be the subject of population analysis (PA) in some localized basis set, $|\psi_{xp}\rangle$. The electronic population of molecule x is usually defined as the expectation value of (a generally non-Hermitian) operator $(\hat{P}_x^{(pa)}\hat{R}_f\hat{P}_x^{(pa)})$:

Downloaded 26 Nov 2008 to 128.32.49.120. Redistribution subject to AIP license or copyright; see http://jcp.aip.org/jcp/copyright.jsp

$$pop_x(\hat{R}_f) = \sum_p^{n_x} \langle \psi^{xp} | \hat{R}_f | \psi_{xp} \rangle = \mathrm{Tr}[\hat{P}_x^{(pa)} \hat{R}_f \hat{P}_x^{(pa)}], \tag{A8}$$

where $|\psi_{xp}\rangle$ denotes basis orbitals and $\hat{P}_x^{(pa)}$ is the partition operator *associated* with the Hilbert subspace of molecule x [Eq. (A1)] that must satisfy the idempotency [Eq. (A2)] and resolution of identity [Eq. (A3)] conditions. The formal charge of molecule x is obtained by summing $pop_x(\hat{R}_f)$ and the nuclear charges of the atoms in the molecule.

If nonorthogonal canonical orbitals of isolated molecules, which define the $\hat{R}_{FRZ}$ state, are used as basis functions, Eq. (A8) represents the Mulliken population analysis (MPA).[34,35] If the basis orbitals are symmetrically orthogonalized then the partiton operators become Hermitian, and Eq. (A8) describes Löwdin population analysis.[36] Weinhold's analysis[49] utilizes a basis set of so-called natural bond orbitals that are orthogonal by construction (expanded in terms of the underlying basis set of occupancy-weighted symmetrically orthogonalized natural atomic orbitals) and can also be described by Eq. (A8). It is important to state that there is no clearly "best" method for allocating a charge distribution among nonorthogonal subspaces associated with orbitals, atoms or molecules. For example, Mulliken analysis can produce orbital populations outside physical range [0,2], whereas in Löwdin analysis the basis functions are not strictly localized after the symmetric orthogonalization is performed (the same is true for natural bond orbitals).

Formal charges on molecules obtained from population analysis do not provide full information about electron reorganization and binding in the system. For example, in a complex with synergic bonding, the analysis of molecular formal charges does not capture full complexity of charge transfer effects in the complex. In population analysis methods, the total charge transfer is calculated as the population of all virtual orbitals in the final state:

$$\begin{aligned} \Delta Q^{(pa)} &\equiv \sum_x pop_x^{(v)}(\hat{R}_f) \\ &= \sum_x \mathrm{Tr}[\hat{V}_x^{(pa)} \hat{R}_f \hat{V}_x^{(pa)}] \\ &= -\sum_x \{\mathrm{Tr}[\hat{O}_x^{(pa)} \hat{R}_f \hat{O}_x^{(pa)}] - o_x\}, \end{aligned} \tag{A9}$$

where partition operators $\hat{O}_x^{(pa)}$ and $\hat{V}_x^{(pa)}$ ($\hat{O}_x^{(pa)} + \hat{V}_x^{(pa)} = \hat{P}_x^{(pa)}$) are *associated* with the occupied and virtual orbitals of molecule x, respectively,

$$\hat{O}_x^{(pa)} = \sum_i^{o_x} |\psi_{xi}\rangle\langle\psi^{xi}|, \tag{A10}$$

$$\hat{V}_x^{(pa)} = \sum_a^{v_x} |\psi_{xa}\rangle\langle\psi^{xa}|. \tag{A11}$$

Note that operators $\hat{O}_x^{(pa)}$ and $\hat{V}_x^{(pa)}$ are not projectors onto the occupied and virtual subspaces. Their sums over all molecules do not give proper projectors either (compare them to operators $\hat{P}_x^{(o)}$ and $\hat{P}_x^{(v)}$ defined in the context of ALMO CTA in Eqs. (A4) and (A5)).

Charge decomposition analysis (CDA)

For systems comprising more than two molecules, it is often important to know not only how much charge is transferred to a molecule but also where it came from, i.e., to find forward donation and backbonding components for *each* pair of molecules in the system. The PA methods are unable to provide this level of detail. In the CDA method of Dapprich and Frenking,[48] the amount of charge transferred from the occupied orbitals on molecule x to the virtual orbitals on molecule y is defined as follows:

$$\begin{aligned} \Delta Q_{\mathrm{occ}(x)\to\mathrm{vir}(y)}^{(\mathrm{CDA})} &= \sum_i^{o_x} \sum_a^{v_y} \langle \psi^{ya} | \hat{R}_f | \psi^{xi} \rangle \sigma_{xi,ya} \\ &= \mathrm{Tr}[\hat{V}_y^{(\mathrm{MPA})} \hat{R}_f (\hat{O}_x^{(\mathrm{MPA})})^\dagger]. \end{aligned} \tag{A12}$$

The basis functions used in CDA are converged canonical orbitals of isolated fragments (FRZ basis) and a Mulliken partitioning (denoted with the MPA superscript) is used.

The CDA has proved useful for comparative studies of charge transfer but there are several problems with adopting such a definition for $\Delta Q_{\mathrm{occ}(x)\to\mathrm{vir}(y)}^{(\mathrm{CDA})}$. First, the CDA definition of the charge transfer components is not consistent with the definition of $\Delta Q^{(\mathrm{MPA})}$ given by Eq. (A9) even though the starting point for deriving the CDA expression is the Mulliken PA,

$$\sum_{x,y} \Delta Q_{\mathrm{occ}(x)\to\mathrm{vir}(y)}^{(\mathrm{CDA})} \neq \Delta Q^{(\mathrm{MPA})}. \tag{A13}$$

Second, it is very hard to assign physical meaning to often large negative terms corresponding to mixing occupied orbitals on one fragment with occupied orbitals on another:

$$\begin{aligned} \Delta Q_{\mathrm{occ}(x)\to\mathrm{occ}(y)}^{(\mathrm{CDA})} &= \sum_i^{o_x} \sum_j^{o_y} \langle \psi^{yj} | \hat{R}_f | \psi^{xi} \rangle \sigma_{xi,yj} \\ &= \mathrm{Tr}[\hat{O}_y^{(\mathrm{MPA})} \hat{R}_f (\hat{O}_x^{(\mathrm{MPA})})^\dagger]. \end{aligned} \tag{A14}$$

The original assignment of these terms to polarization effects does not agree with a widely accepted view that polarization effects correspond to occupied-virtual orbital mixing within a molecule. Even though the reference orbitals are not optimized for intrafragment relaxation in CDA, intrafragment occupied-virtual charge transfer terms are always zero in this method. This is because orbitals within a molecule can always be orthogonalized thus giving zero σ matrix elements in Eq. (A12) for $\Delta Q_{\mathrm{occ}(x)\to\mathrm{vir}(x)}^{(\mathrm{CDA})}$.

Third, large intermolecular virtual-virtual terms ($\Delta Q_{\mathrm{vir}(x)\to\mathrm{vir}(y)}^{(\mathrm{CDA})}$) and (generally small) intramolecular virtual-virtual ($\Delta Q_{\mathrm{vir}(x)\to\mathrm{vir}(x)}^{(\mathrm{CDA})}$) do not have a clear physical meaning either.

Finally, CDA does not produce correct charge transfer results in the limit of orthogonal basis orbitals because of the direct inclusion of the overlap matrix into each charge transfer term. Therefore, zero charge transfer is produced for *any*

Downloaded 26 Nov 2008 to 128.32.49.120. Redistribution subject to AIP license or copyright; see http://jcp.aip.org/jcp/copyright.jsp

density matrix, $\hat{R}_f$, for all methods in which virtual orbitals are orthogonal to the occupied orbitals, and for all systems in which charge transfer occurs between spatially separated fragments.

Most importantly population analysis and CDA methods do not define occupied and virtual subspaces for the reference state and, therefore, produce electron density reorganization effects without corresponding well defined energies of charge transfer.

[1] J.-M. Lehn, *Supramolecular Chemistry: Concepts and Perspectives* (VCH, Weinheim, 1995).
[2] J. W. Steed and J. L. Atwood, *Supramolecular Chemistry* (Wiley, New York, 2000).
[3] G. Desiraju and T. Steiner, *The Weak Hydrogen Bond in Structural Chemistry and Biology* (Oxford University Press, New York, 1999).
[4] G. A. Jeffrey, *An Introduction to Hydrogen Bonding* (Oxford University Press, Oxford, 1997).
[5] S. Scheiner, *Hydrogen Bonding: A Theoretical Perspective* (Oxford University Press, Oxford, 1997).
[6] A. van der Vaart and K. M. Merz, J. Am. Chem. Soc. **121**, 9182 (1999).
[7] A. van der Vaart and K. M. Merz, Int. J. Quantum Chem. **77**, 27 (2000).
[8] *Comprehensive Coordination Chemistry: The Synthesis, Reactions, Properties, and Applications of Coordination Compounds*, edited by G. Wilkinson, R. Gillard, and J. McCleverty (Pergamon, New York, 1987).
[9] Y. Jean, *Molecular Orbitals of Transition Metal Complexes* (Oxford University Press, Oxford, 2005).
[10] A. E. Shilov, *Metal Complexes in Biomimetic Chemical Reactions:* N_2 *Fixation in Solution, Activation, and Oxidation of Alkanes, Chemical Models of Photosynthesis* (CRC, Boca Raton, New York, 1997).
[11] G. J. Kubas, *Metal Dihydrogen and σ-bond Complexes: Structure, Theory and Reactivity* (Kluwer, New York, 2002).
[12] *Theoretical Aspects of Homogeneous Catalysis: Applications of ab initio Molecular Orbital Theory*, edited by P. van Leeuwen, K. Morokuma, and J. H. van Lenth (Kluwer, Boston, 1995).
[13] A. J. Stone, *The Theory of Intermolecular Forces* (Oxford University Press, New York, 1996).
[14] K. Kitaura and K. Morokuma, Int. J. Quantum Chem. **10**, 325 (1976).
[15] W. J. Stevens and W. H. Fink, Chem. Phys. Lett. **139**, 15 (1987).
[16] W. Chen and M. S. Gordon, J. Phys. Chem. **100**, 14316 (1996).
[17] P. S. Bagus, K. Hermann, and C. W. Bauschlicher, J. Chem. Phys. **80**, 4378 (1984).
[18] P. S. Bagus and F. Illas, J. Chem. Phys. **96**, 8962 (1992).
[19] E. D. Glendening and A. Streitwieser, J. Chem. Phys. **100**, 2900 (1994).
[20] G. K. Schenter and E. D. Glendening, J. Phys. Chem. **100**, 17152 (1996).
[21] E. D. Glendening, J. Phys. Chem. A **109**, 11936 (2005).
[22] Y. Mochizuki, K. Fukuzawa, A. Kato, S. Tanaka, K. Kitaura, and T. Nakano, Chem. Phys. Lett. **410**, 247 (2005).
[23] J. Korchowiec and T. Uchimaru, J. Chem. Phys. **112**, 1623 (2000).
[24] A. van der Vaart and K. M. Merz, J. Phys. Chem. A **103**, 3321 (1999).
[25] Y. R. Mo, J. L. Gao, and S. D. Peyerimhoff, J. Chem. Phys. **112**, 5530 (2000).
[26] R. Z. Khaliullin, E. A. Cobar, R. C. Lochan, A. T. Bell, and M. Head-Gordon, J. Phys. Chem. A **111**, 8753 (2007).
[27] R. Bader, *Atoms in Molecules: A Quantum Theory* (Oxford University Press, New York, 1994).
[28] E. Francisco, A. M. Pendas, and M. A. Blanco, J. Chem. Theory Comput. **2**, 90 (2006).
[29] A. D. Becke and K. E. Edgecombe, J. Chem. Phys. **92**, 5397 (1990).
[30] A. Savin, R. Nesper, S. Wengert, and T. F. Fassler, Angew. Chem., Int. Ed. Engl. **36**, 1809 (1997).
[31] B. Silvi and A. Savin, Nature (London) **371**, 683 (1994).
[32] F. L. Hirshfeld, Theor. Chim. Acta **44**, 129 (1977).
[33] A. E. Reed, R. B. Weinstock, and F. Weinhold, J. Chem. Phys. **83**, 735 (1985).
[34] R. S. Mulliken, J. Chem. Phys. **23**, 1833 (1955).
[35] R. S. Mulliken, J. Chem. Phys. **23**, 1841 (1955).
[36] P. O. Lowdin, J. Chem. Phys. **18**, 365 (1950).
[37] K. E. Edgecombe and R. J. Boyd, J. Chem. Soc., Faraday Trans. 2 **83**, 1307 (1987).
[38] K. R. Roby, Mol. Phys. **27**, 81 (1974).
[39] K. R. Roby, Mol. Phys. **28**, 1441 (1974).
[40] J. Pipek, J. Mol. Struct.: THEOCHEM **501**, 395 (2000).
[41] R. Z. Khaliullin, M. Head-Gordon, and A. T. Bell, J. Chem. Phys. **124**, 204105 (2006).
[42] H. Stoll, G. Wagenblast, and H. Preuss, Theor. Chim. Acta **57**, 169 (1980).
[43] J. M. Cullen, Int. J. Quantum Chem., Quantum Chem. Symp. **25**, 193 (1991).
[44] E. Gianinetti, M. Raimondi, and E. Tornaghi, Int. J. Quantum Chem. **60**, 157 (1996).
[45] T. Nagata, O. Takahashi, K. Saito, and S. Iwata, J. Chem. Phys. **115**, 3553 (2001).
[46] A. Fornili, M. Sironi, and M. Raimondi, J. Mol. Struct.: THEOCHEM **632**, 157 (2003).
[47] M. Sironi, A. Genoni, M. Civera, S. Pieraccini, and M. Ghitti, Theor. Chem. Acc. **117**, 685 (2007).
[48] S. Dapprich and G. Frenking, J. Phys. Chem. **99**, 9352 (1995).
[49] J. P. Foster and F. Weinhold, J. Am. Chem. Soc. **102**, 7211 (1980).
[50] J. S. Dewar, Bull. Soc. Chim. Fr. **18**, C71 (1951).
[51] J. Chatt and L. A. Duncanson, J. Chem. Soc., 2929 (1953).
[52] W. Z. Liang and M. Head-Gordon, J. Phys. Chem. A **108**, 3206 (2004).
[53] W. Z. Liang and M. Head-Gordon, J. Chem. Phys. **120**, 10379 (2004).
[54] I. Mayer and A. Hamza, Int. J. Quantum Chem. **103**, 798 (2005).
[55] S. F. Boys and F. Bernardi, Mol. Phys. **19**, 553 (1970).
[56] Y. Shao, L. F. Molnar, Y. Jung, J. Kussmann, C. Ochsenfeld, S. T. Brown, A. T. B. Gilbert, L. V. Slipchenko, S. V. Levchenko, D. P. O'Neill, R. A. DiStasio, R. C. Lochan, T. Wang, G. J. O. Beran, N. A. Besley, J. M. Herbert, C. Y. Lin, T. Van Voorhis, S. H. Chien, A. Sodt, R. P. Steele, V. A. Rassolov, P. E. Maslen, P. P. Korambath, R. D. Adamson, B. Austin, J. Baker, E. F. C. Byrd, H. Dachsel, R. J. Doerksen, A. Dreuw, B. D. Dunietz, A. D. Dutoi, T. R. Furlani, S. R. Gwaltney, A. Heyden, S. Hirata, C. P. Hsu, G. Kedziora, R. Z. Khalliulin, P. Klunzinger, A. M. Lee, M. S. Lee, W. Liang, I. Lotan, N. Nair, B. Peters, E. I. Proynov, P. A. Pieniazek, Y. M. Rhee, J. Ritchie, E. Rosta, C. D. Sherrill, A. C. Simmonett, J. E. Subotnik, H. L. Woodcock, W. Zhang, A. T. Bell, A. K. Chakraborty, D. M. Chipman, F. J. Keil, A. Warshel, W. J. Hehre, H. F. Schaefer, J. Kong, A. I. Krylov, P. M. W. Gill, and M. Head-Gordon, Phys. Chem. Chem. Phys. **8**, 3172 (2006).
[57] G. N. Lewis, J. Franklin Inst. **226**, 293 (1938).
[58] R. G. Pearson, J. Am. Chem. Soc. **85**, 3533 (1963).
[59] H. L. Finston and A. C. Rychtman, *A New View of Current Acid-Base Theories* (Wiley, New York, 1982).
[60] D. R. Lloyd and N. Lynaugh, J. Chem. Soc., Faraday Trans. 2 **68**, 947 (1972).
[61] D. B. Beach and W. L. Jolly, Inorg. Chem. **24**, 567 (1985).
[62] W. C. Ermler, F. D. Glasser, and C. W. Kern, J. Am. Chem. Soc. **98**, 3799 (1976).
[63] C. W. Bauschlicher and A. Ricca, Chem. Phys. Lett. **237**, 14 (1995).
[64] V. Jonas, G. Frenking, and M. T. Reetz, J. Am. Chem. Soc. **116**, 8741 (1994).
[65] S. Erhardt and G. Frenking, Chem.-Eur. J. **12**, 4620 (2006).
[66] Y. R. Mo, L. C. Song, W. Wu, and Q. N. Zhang, J. Am. Chem. Soc. **126**, 3974 (2004).
[67] C. S. Brauer, M. B. Craddock, J. Kilian, E. M. Grumstrup, M. C. Orilall, Y. R. Mo, J. L. Gao, and K. R. Leopold, J. Phys. Chem. A **110**, 10025 (2006).
[68] Y. R. Mo and J. L. Gao, J. Phys. Chem. A **105**, 6530 (2001).
[69] M. B. Hall and R. F. Fenske, Inorg. Chem. **11**, 768 (1972).
[70] F. Aubke and C. Wang, Coord. Chem. Rev. **137**, 483 (1994).
[71] M. A. Lynn and B. E. Bursten, Inorg. Chim. Acta **229**, 437 (1995).
[72] A. J. Lupinetti, S. H. Strauss, and G. Frenking, Prog. Inorg. Chem. **49**, 1 (2001).
[73] S. H. Strauss, J. Chem. Soc. Dalton Trans. 1 (2000).
[74] A. J. Lupinetti, G. Frenking, and S. H. Strauss, Angew. Chem., Int. Ed. **37**, 2113 (1998).
[75] C. A. Brown, K. S. Jeong, R. H. Poppenga, B. Puschner, D. M. Miller, A. E. Ellis, K. I. Kang, S. Sum, A. M. Cistola, and S. A. Brown, J. Vet. Diagn. Invest **19**, 525 (2007).
[76] See: http://www.avma.org/press/releases/070501_petfoodrecall.asp.
[77] R. Z. Khaliullin, M. Head-Gordon, and A. T. Bell, J. Phys. Chem. B **111**, 10992 (2007).
[78] E. A. Cobart, R. Z. Khaliullin, R. G. Bergman, and M. Head-Gordon, Proc. Natl. Acad. Sci. U.S.A. **104**, 6963 (2007).
[79] R. C. Lochan, R. Z. Khaliullin, and M. Head-Gordon, Inorg. Chem. **47**, 4032 (2008).

Downloaded 26 Nov 2008 to 128.32.49.120. Redistribution subject to AIP license or copyright; see http://jcp.aip.org/jcp/copyright.jsp